

## A point-by-point response to the reviews

We are very thankful to two reviewers for your valuable comments and thoughtful suggestions. The followings are our responses to your comments. The comments of the reviewers are shown in black, our responses to the comments are presented in blue, and the new or modified texts are provided in blue in *italics*.

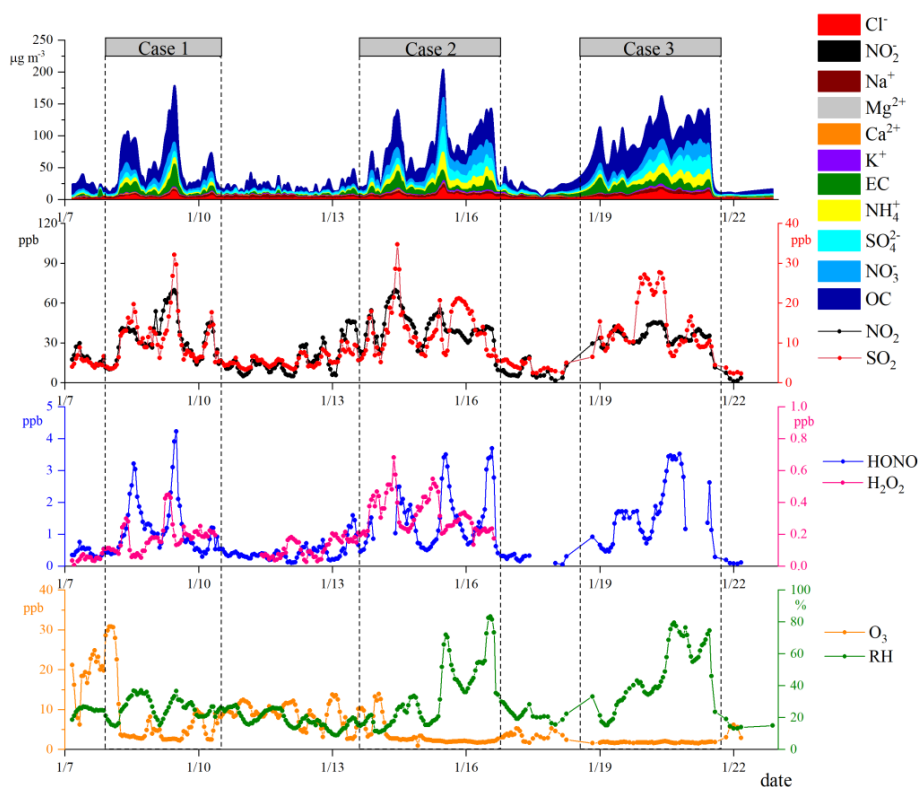
### Response to Reviewer #1

**Comment 1:** This study investigates the pollution characteristics and formation mechanisms of sulfate and nitrate during the winter haze pollution periods in Beijing in 2016 based on the field observations, which is helpful for us to understand the winter haze formation in China and better control it. However, some discussions are confusing. This paper cannot be accepted before the authors have addressed the following comments.

**Answer:** Thank you for your pertinent evaluation of our work. The followings are our responses to your comments.

**Comment 2:** Line 257-258: The variation of NO<sub>2</sub> should be given in Figure 1, because the discussion in this study is based on NO<sub>2</sub>, not NO<sub>x</sub>. Are the concentrations of SO<sub>2</sub> a factor of 5 lower than the concentrations of NO<sub>2</sub>? Based on Table 1, it's not true.

**Answer:** The time series of NO<sub>x</sub> have been replaced with the variations of NO<sub>2</sub> in the revised Figure 1 (Figure R1). On the basis of Figure R1 and Table 1, the concentrations of SO<sub>2</sub> were about a factor of 5-6 lower than those of NO<sub>x</sub>, but were approximately a factor of 3 lower than those of NO<sub>2</sub>. This sentence has been changed in the revised manuscript as following:

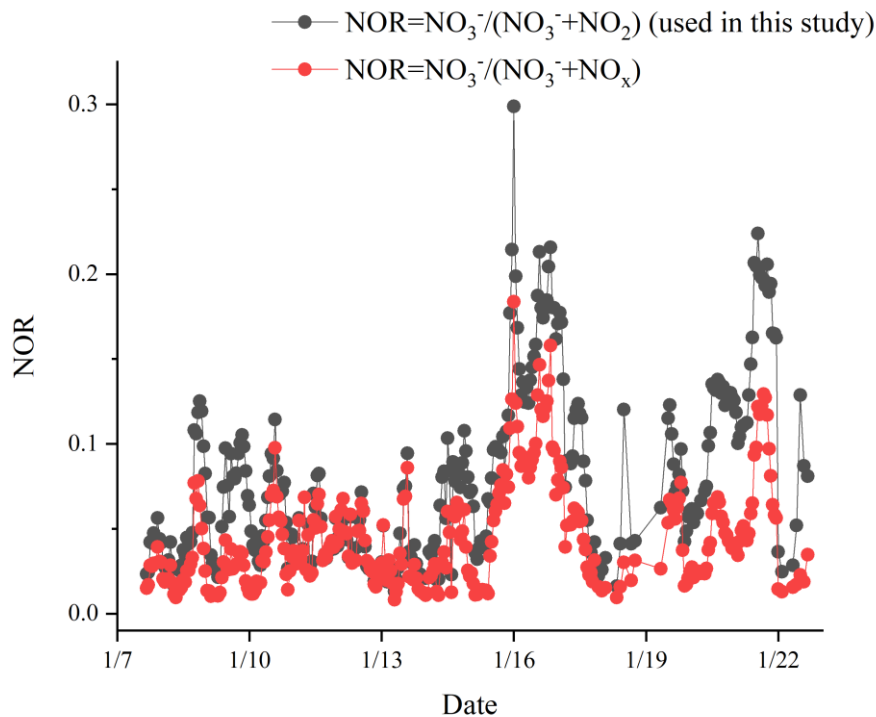


26 **Figure R1.** Time series of the species in PM<sub>2.5</sub> and typical gaseous pollutants (NO<sub>2</sub>, SO<sub>2</sub>, O<sub>3</sub>,  
27 HONO and H<sub>2</sub>O<sub>2</sub>) as well as atmospheric RH during the sampling period.  
28

29 *“Although the concentrations of SO<sub>2</sub> were obviously lower than the concentrations of NO<sub>2</sub> in both  
30 Case 2 and Case 3 (Figure 1 and Table 1), ...”*  
31

32 **Comment 3:** Line 262: NOR is commonly defined as “NOR = NO<sub>3</sub><sup>-</sup> / (NO<sub>3</sub><sup>-</sup>+NO<sub>2</sub>)” in the previous  
33 studies. Why is “NOR = NO<sub>3</sub><sup>-</sup> / (NO<sub>3</sub><sup>-</sup>+NO<sub>x</sub>)” used in this study? We know that NO<sub>x</sub> is usually much  
34 higher than NO<sub>2</sub>, especially at night. Are the discussion and results different if you use “NOR =  
35 NO<sub>3</sub><sup>-</sup> / (NO<sub>3</sub><sup>-</sup>+NO<sub>2</sub>)” in this study? If you use “NOR = NO<sub>3</sub><sup>-</sup> / (NO<sub>3</sub><sup>-</sup>+NO<sub>2</sub>)”, why do you use “NO<sub>2</sub> ×  
36 O<sub>3</sub>”, “Dust × NO<sub>2</sub>” and “HONO × DR × NO<sub>2</sub>” in the following discussion, rather than “NO<sub>x</sub> × O<sub>3</sub>”,  
37 “Dust × NO<sub>x</sub>” and “HONO × DR × NO<sub>x</sub>”?  
38

39 **Answer:** We are very sorry for our incorrect writing of the NOR formula. In fact, “NOR = NO<sub>3</sub><sup>-</sup> /  
40 (NO<sub>3</sub><sup>-</sup>+NO<sub>2</sub>)” rather than “NOR = NO<sub>3</sub><sup>-</sup> / (NO<sub>3</sub><sup>-</sup>+NO<sub>x</sub>)” was used in this study. As NO concentration  
41 usually accounted for relatively high fraction to that of NO<sub>x</sub> in winter of Beijing city, especially  
42 during the morning and evening rushing hours, NOR calculated based on NO<sub>2</sub> was obviously higher  
43 than that based on NO<sub>x</sub> (Figure R2). Because atmospheric nitrate is formed through the oxidation  
44 of NO<sub>2</sub> via gas-phase, heterogeneous and aqueous-phase reactions, “NOR = NO<sub>3</sub><sup>-</sup> / (NO<sub>3</sub><sup>-</sup>+NO<sub>2</sub>)”  
45 might reflect nitrogen oxidation ratio more accurately than “NOR = NO<sub>3</sub><sup>-</sup> / (NO<sub>3</sub><sup>-</sup>+NO<sub>x</sub>)”. The  
46 mistake has been corrected in the revised manuscript as following:



47  
48 **Figure R2.** The comparison of the time series of NOR calculated based on NO<sub>2</sub> and NO<sub>x</sub> during  
49 the sampling period.  
50

51 *“To further investigate the pollution characteristics of nitrate and sulfate during the serious*  
52 *pollution episodes, the relations between NOR ( $NOR = NO_3^- / (NO_3^- + NO_2)$ ) as well as SOR ( $SOR$*   
53  *$= SO_4^{2-} / (SO_4^{2-} + SO_2)$ ) and RH are shown in Figure 2.”*

54

55 **Comment 4:** Line 270-271: Why is the reduction of NOR due to the deliquescence of nitrate? Based  
56 on the reference you list, the deliquescence can change aerosol particle size distribution, but not  
57 decrease the nitrate concentration.

58

59 **Answer:** According to the Comment 4 from the Reviewer #2, the reduction of NOR might be  
60 ascribed to the suppressed heterogeneous reactions of  $NO_2$  to nitrate formation under high RH  
61 condition (Tang et al., 2017). The heterogeneous reactions of  $NO_2$  on particle surface have been  
62 found to be dependent on atmospheric RH due to the competition of water for surface reactive sites  
63 of particles (Ponczek et al., 2019), and thus relatively fast nitrate formation usually occurs when RH  
64 is below a certain value. This sentence has been rephrased in the revised manuscript as following:

65

66 *“the variation trend of NOR slowly decreased whereas the variation trend of SOR significantly*  
67 *increased when atmospheric RH was above 60 %, which was very similar with the previous studies*  
68 *(Sun et al., 2013; Zheng et al., 2015b). Considering that the heterogeneous reactions of  $NO_2$  on*  
69 *particle surface were dependent on atmospheric RH due to the competition of water for surface*  
70 *reactive sites of particles (Ponczek et al., 2019), the slow reduction of NOR might be due to the*  
71 *suppressed heterogeneous reaction of  $NO_2$  to nitrate formation under high RH condition (Tang et*  
72 *al., 2017), while the elevation of SOR revealed the dominant contribution of the aqueous-phase*  
73 *reaction to sulfate formation.”*

74

75 **Comment 5:** Section 3.3.1: The discussion about the nitrate formation is not convincing and more  
76 analysis is needed.

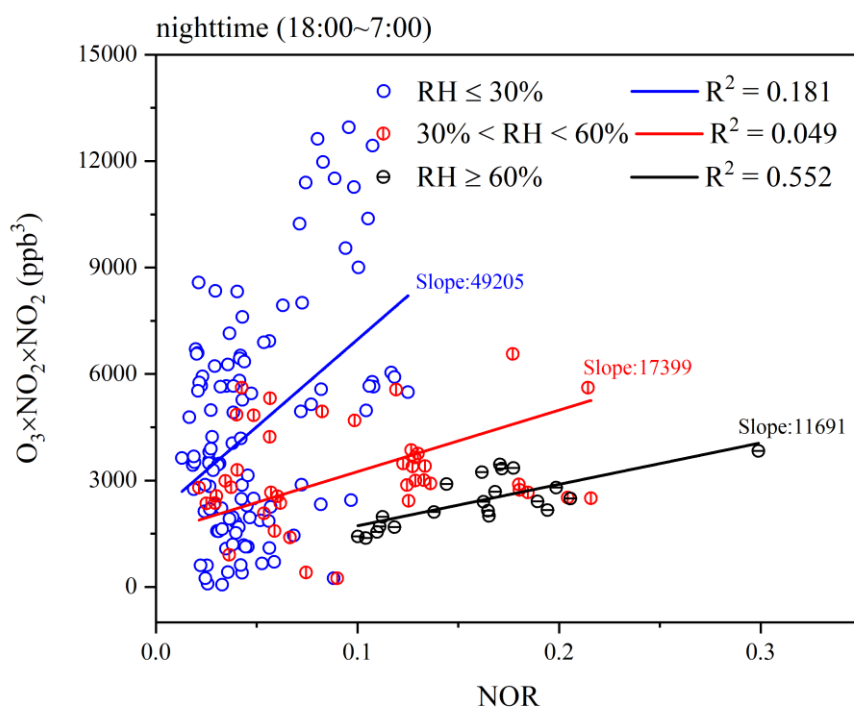
77 (1) Line 295-299: Is the correlation analysis in Figure 3b proper to investigate the contribution of  
78 heterogeneous hydrolysis of  $N_2O_5$ ? Why does a negative correlation exist between NOR and  $NO_2$   
79  $\times O_3$  under the  $RH < 60\%$  condition? It means that the heterogeneous hydrolysis of  $N_2O_5$  is not  
80 important under the  $RH < 60\%$  condition? If the authors use a similar figure with Figure 3b to  
81 analyze the correlation between NOR with  $Dust \times NO_2$  and  $HONO \times DR \times NO_2$ , what are the  
82 conclusion?

83

84 **Answer:** Considering that one molecule of  $N_2O_5$  could be generated by two molecule of  $NO_2$   
85 reacting with one molecule of  $O_3$ , perhaps it's more proper to use the correlation between NOR and  
86  $[NO_2]^2 \times [O_3]$  rather than  $[NO_2] \times [O_3]$  for representing the contribution of the heterogeneous  
87 hydrolysis of  $N_2O_5$  to atmospheric nitrate at night (the Comment 5 from the Reviewer #2). The  
88 correlations between NOR and  $[NO_2]^2 \times [O_3]$  at the nighttime (redefined as 18:00-7:00) under  
89 different RH conditions are shown in Figure R3. It's evident that the variations of  $[NO_2]^2 \times [O_3]$   
90 were all positively correlated with NOR under the three different RH conditions, and their  
91 correlation under the  $RH \geq 60\%$  condition ( $R^2 = 0.552$ ) was significantly stronger than those under  
92 the  $RH < 60\%$  condition ( $R^2 \leq 0.181$ ). It has been acknowledged that the correlation between two  
93 species means the impact of changes in one species on another. The stronger the correlation is, the  
94 greater the impact is. Therefore, the positive correlations between NOR and  $[NO_2]^2 \times [O_3]$  indicated

95 that the heterogeneous hydrolysis of  $N_2O_5$  could contribute to the formation of atmospheric nitrate  
 96 at the nighttime under different RH conditions. The significantly stronger correlations between NOR  
 97 and  $[NO_2]^2 \times [O_3]$  under the  $RH \geq 60\%$  condition than under the  $RH < 60\%$  condition revealed that  
 98 the heterogeneous hydrolysis of  $N_2O_5$  made a remarkable contribution to atmospheric nitrate at the  
 99 nighttime under high RH condition. Additionally, the obviously lower slope of the correlation  
 100 between NOR and  $[NO_2]^2 \times [O_3]$  under the  $RH \geq 60\%$  condition (slope = 11691) than under the  $RH$   
 101  $< 60\%$  condition (slope  $\geq 17399$ ) also suggested that the formation of atmospheric nitrate at the  
 102 nighttime under high RH condition was more sensitive to the pathway of  $N_2O_5$ . These sentences  
 103 have been modified in the revised manuscript as stated above.

104 It should be noted that the correlations between NOR and  $[NO_2]^2 \times [O_3]$  under the three  
 105 different RH conditions were analyzed for verifying under which RH condition the heterogeneous  
 106 hydrolysis of  $N_2O_5$  made a remarkable contribution to atmospheric nitrate at the nighttime, while  
 107 the daily variations of  $[Dust] \times [NO_2]$  and  $[HONO] \times [DR] \times [NO_2]$  under the  $30\% < RH < 60\%$   
 108 condition were compared for exploring which reaction could play an important role in atmospheric  
 109 nitrate at the daytime under moderate RH condition. Therefore, it may be lack of the purpose to  
 110 analyze the correlations between NOR and  $[Dust] \times [NO_2]$  as well as  $[HONO] \times [DR] \times [NO_2]$  by  
 111 using the similar method of Figure R3.

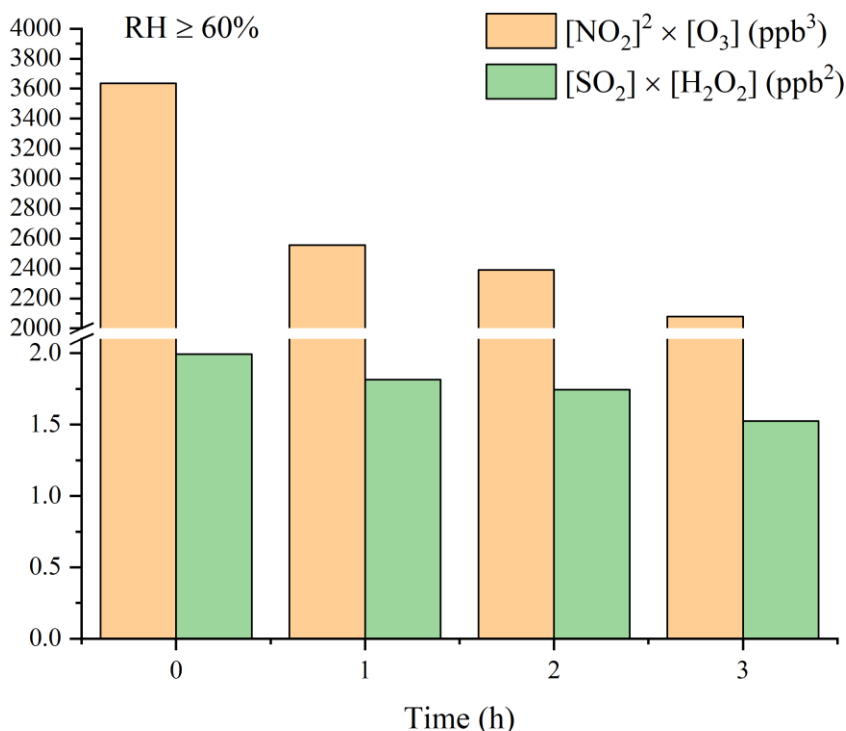


112  
 113 **Figure R3.** The correlations between NOR and  $[NO_2]^2 \times [O_3]$  at the nighttime under different RH  
 114 conditions.  
 115

116 (2) Figure 3a: Why does NOR decrease obviously during 0:00-4:00 under the  $RH > 60\%$  condition?  
 117

118 **Answer:** As mentioned above, the heterogeneous hydrolysis of  $N_2O_5$  was found to make a  
 119 remarkable contribution to atmospheric nitrate at the nighttime under the  $RH \geq 60\%$  condition due

120 to the strong correlation between NOR and  $[\text{NO}_2]^2 \times [\text{O}_3]$ . Thus, the obvious reduction of the NOR  
 121 values during 0:00-3:00 under the  $\text{RH} \geq 60\%$  condition was mainly ascribed to the decrease in the  
 122 concentration levels of  $[\text{NO}_2]^2 \times [\text{O}_3]$  (Figure R4).



123  
 124 **Figure R4.** The variations of  $[\text{NO}_2]^2 \times [\text{O}_3]$  and  $[\text{SO}_2] \times [\text{H}_2\text{O}_2]$  during 0:00-3:00 under the  $\text{RH} \geq$   
 125 60% condition during the sampling period.  
 126

127 (3) Line 296-297: why is the nighttime defined as 19:00-6:00? Seeing from Figure 3d, DR is nearly  
 128 zero during 18:00-7:00.

129  
 130 **Answer:** Thank you for your suggestion. The nighttime has been redefined as 18:00-7:00 and the  
 131 associated figures have been changed in the revised manuscript.

132  
 133 (4) Line 300-302: A similar NOR increase during the daytime can be seen under the  $\text{RH} > 60\%$   
 134 condition in Figure 3a. Why are the hourly variations of  $\text{Dust} \times \text{NO}_2$  and  $\text{HONO} \times \text{DR} \times \text{NO}_2$  under  
 135 the  $\text{RH} > 60\%$  condition not included in Figure 3c-d. Seeing from the abstract (Line 27-30) and  
 136 conclusion part (Line 365-368), the authors seem to conclude the gas-phase reaction of  $\text{NO}_2$  with  
 137 OH plays a key role just under moderate RH conditions. How about under the  $\text{RH} > 60\%$  or  $\text{RH} < 30\%$   
 138 condition?

139  
 140 **Answer:** The relatively high atmospheric RH ( $\text{RH} > 60\%$ ) usually occurred at the nighttime during  
 141 the sampling period (Figure R4), and hence it was difficult by using  $[\text{HONO}] \times [\text{DR}] \times [\text{NO}_2]$  to  
 142 conclude whether the gas-phase reaction of  $\text{NO}_2$  with OH played a key role under the  $\text{RH} > 60\%$   
 143 condition. Furthermore, because the NOR values under the  $\text{RH} \leq 30\%$  condition were almost less

144 than 0.1 (Figure 2 in the revised manuscript) which reflected no occurrence of secondary formation  
145 of nitrate (Gao et al., 2011; Zhang et al., 2018), it might be not necessary to discuss the formation  
146 of nitrate under the  $RH \leq 30\%$  condition.

147

148 **Comment 6:** Section 3.3.2:

149 (1) Line 325-328: Why is the heterogeneous reaction of  $SO_2$  on the surface of mineral aerosols not  
150 important before 14:00?

151

152 **Answer:** Atmospheric sulfate has been reported to come mainly from primary source emissions  
153 when the SOR is less than 0.1 (Gao et al., 2011; Zhang et al., 2018). Considering that the mean  
154 values of SOR before 14:00 both under the  $30\% < RH < 60\%$  and  $RH \leq 30\%$  conditions were almost  
155 close to 0.1, secondary formation of  $SO_2$  including the gas-phase reaction and heterogeneous  
156 reaction could be ignored before 14:00. To avoid possible confusing understanding for readers, this  
157 sentence has been rephrased in the revised manuscript as following:

158

159 *“As shown in Figure 4, similar to the daily variations of NOR, the mean values of SOR were found*  
160 *to elevated remarkably under the  $30\% < RH < 60\%$  condition compared to the  $RH \leq 30\%$  condition,*  
161 *especially during 14:00-22:00, which might be mainly ascribed to the enhanced gas-phase reaction*  
162 *and the heterogeneous reaction of  $SO_2$  involving aerosol liquid water under the relatively high RH*  
163 *condition.”*

164

165 (2) Figure 4: Why does SOR decrease obviously during 0:00-4:00 under the  $RH > 60\%$  condition?

166

167 **Answer:** Because the oxidation of  $SO_2$  through the aqueous-phase reaction of  $H_2O_2$  was found to  
168 contribute mainly to sulfate formation under the high RH condition, the depletion of the oxidant and  
169 the precursor ( $[SO_2] \times [H_2O_2]$ ) during 0:00-3:00 was suspected to result in the obvious decrease of  
170 SOR under the  $RH \geq 60\%$  condition (Figure R4).

171

172 (3) Figure 4: Under  $30\% < RH < 60\%$ , why is the SOR during 13:00-23:00 much higher than that in  
173 other hours? We know that RH is commonly high at night, for example during 0:00-5:00.

174

175 **Answer:** Yes. atmospheric RH is indeed a key factor for influencing sulfate formation and  
176 commonly high at night. Except for atmospheric RH, the concentrations of the precursors such as  
177  $SO_2$  could also play a vital role in the formation of sulfate, and then affected SOR value. Therefore,  
178 the much higher mean values of SOR during 13:00-23:00 than those in other hours might be mainly  
179 attributed to the relatively high concentrations of  $SO_2$  during 13:00-23:00 under  $30\% < RH < 60\%$   
180 condition (Figure R5).

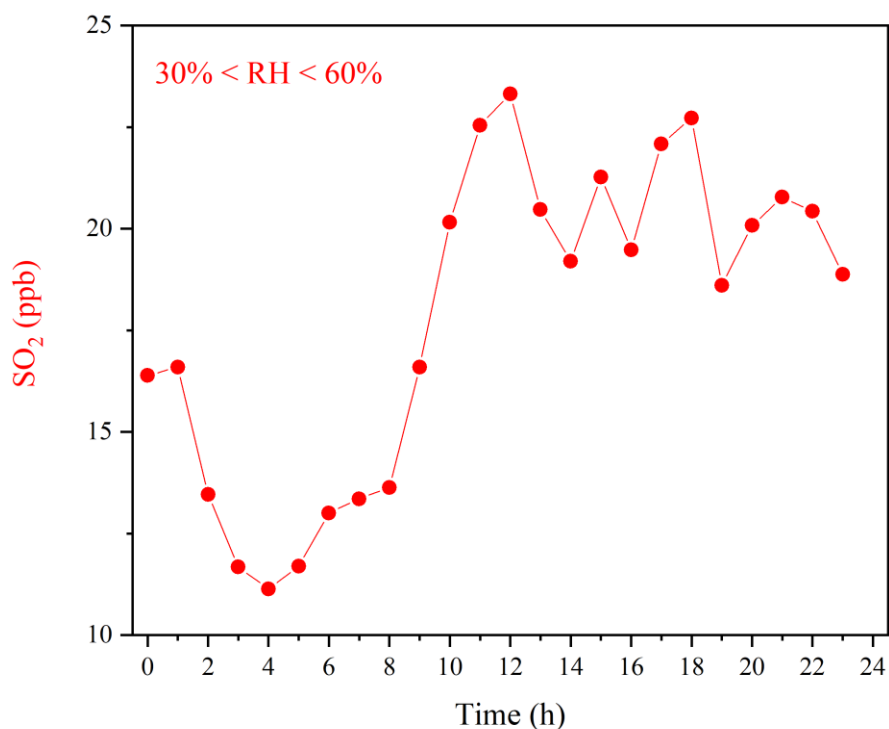


**Figure R5.** The daily variation of SO<sub>2</sub> under the 30% < RH < 60% condition during the sampling period

**Response to Reviewer #2**

**Comment 1:** This study focused on the formation mechanisms of nitrate and sulfate in Beijing, especially the different mechanisms under various RH conditions. The heterogeneous hydrolysis of N<sub>2</sub>O<sub>5</sub> was responsible for the nocturnal formation of nitrate at extremely high RH levels (RH>60 %), while homogeneous reaction between NO<sub>2</sub> and OH radical dominated the formation under moderate condition (30 %<RH<60 %). For SO<sub>4</sub><sup>2-</sup>, aqueous reaction between SO<sub>2</sub> and H<sub>2</sub>O<sub>2</sub> attributed to its formation under high RH condition. The target of this study is meaningful to understanding the formation mechanism of nitrate and sulfate in real atmosphere. There are several questions not very clear.

**Answer:** Thank you for your valuable evaluation of our work. The followings are our responses to your comments.

**Comment 2:** Please give a brief description of NOR and SOR in abstract.

**Answer:** the NOR and SOR formulas have been added in the revised abstract.

**Comment 3:** Did NOR and SOR represent the secondary formation of NO<sub>3</sub><sup>-</sup> and SO<sub>4</sub><sup>2-</sup>, respectively? Actually, when NO<sub>x</sub> and SO<sub>2</sub> reached zero, the value of NOR and SOR were closed to the maximum. If NOR and SOR represent the secondary formation of NO<sub>3</sub><sup>-</sup> and SO<sub>4</sub><sup>2-</sup>, secondary formation of NO<sub>3</sub><sup>-</sup>

205 and  $\text{SO}_4^{2-}$  showed up with low concentration of  $\text{NO}_x$  and  $\text{SO}_2$ . This result is confusing.

206

207 **Answer:** NOR ( $\text{NOR} = \text{NO}_3^- / (\text{NO}_3^- + \text{NO}_2)$ ) and SOR ( $\text{SOR} = \text{SO}_4^{2-} / (\text{SO}_4^{2-} + \text{SO}_2)$ ) didn't represent  
208 the secondary formation of  $\text{NO}_3^-$  and  $\text{SO}_4^{2-}$ , but could reflect their formation potentials to a certain  
209 degree due to the ratios counteracted the air diffusion effect on their concentrations, and thus NOR  
210 and SOR have been widely used to estimate the secondary formation of  $\text{NO}_3^-$  and  $\text{SO}_4^{2-}$ , respectively  
211 (Zheng et al., 2015). Yes, the NOR and SOR would be close to the maximal values if  $\text{NO}_2$  and  $\text{SO}_2$   
212 reached zero. Actually,  $\text{NO}_2$  and  $\text{SO}_2$  are ubiquitous trace gases in the atmosphere, it is impossible  
213 that their concentrations reached zero. The values of NOR and SOR mainly depend on the  
214 conversion efficiencies of  $\text{NO}_2$  and  $\text{SO}_2$  to nitrate and sulfate through various atmospheric chemical  
215 reactions, rather than the concentrations of  $\text{NO}_2$  and  $\text{SO}_2$ , because the concentrations of  $\text{NO}_2$ ,  $\text{SO}_2$ ,  
216 nitrate and sulfate usually have the similar variation trends which are mainly governed by  
217 meteorological conditions and boundary layer heights as well.

218

219 **Comment 4:** The authors mentioned that "The reduction of NOR might be due to the deliquescence  
220 of nitrate at atmospheric RH around 60 %" at line 270-271. However, the deliquescence of nitrate  
221 would not reduce the nitrate in particle but change its phase state. RH has been validated to affect  
222 the heterogeneous reaction of  $\text{NO}_x$  and HONO, which may result in the reduction of nitrate at high  
223 RH condition.

224

225 **Answer:** Thank you for your valuable comment. According to your suggestion, this sentence has  
226 been rephrased in the revised manuscript as following:

227

228 *"the variation trend of NOR slowly decreased whereas the variation trend of SOR significantly*  
229 *increased when atmospheric RH was above 60 %, which was very similar with the previous studies*  
230 *(Sun et al., 2013; Zheng et al., 2015b). Considering that the heterogeneous reactions of  $\text{NO}_2$  on*  
231 *particle surface were dependent on atmospheric RH due to the competition of water for surface*  
232 *reactive sites of particles (Ponczek et al., 2019), the slow reduction of NOR might be due to the*  
233 *suppressed heterogeneous reaction of  $\text{NO}_2$  to nitrate formation under high RH condition (Tang et*  
234 *al., 2017), while the elevation of SOR revealed the dominant contribution of the aqueous-phase*  
235 *reaction to sulfate formation."*

236

237 **Comment 5:** One  $\text{N}_2\text{O}_5$  could be generated by two  $\text{NO}_2$  reacting with one  $\text{O}_3$ . Hence, is it more  
238 suitable to use  $[\text{NO}_2]^2 \times [\text{O}_3]$  rather than  $[\text{NO}_2] \times [\text{O}_3]$  for representing the heterogeneous hydrolysis  
239 of  $\text{N}_2\text{O}_5$  to atmospheric nitrate at night?

240

241 **Answer:** Thank you for your valuable suggestion. Relevant figure (Figure R3) and sentences have  
242 been modified accordingly in the revised manuscript as following:

243

244 *"...Therefore, the correlation between  $[\text{NO}_2]^2 \times [\text{O}_3]$  and NOR can represent roughly the*  
245 *contribution of the heterogeneous hydrolysis of  $\text{N}_2\text{O}_5$  to atmospheric nitrate at night..."*

246

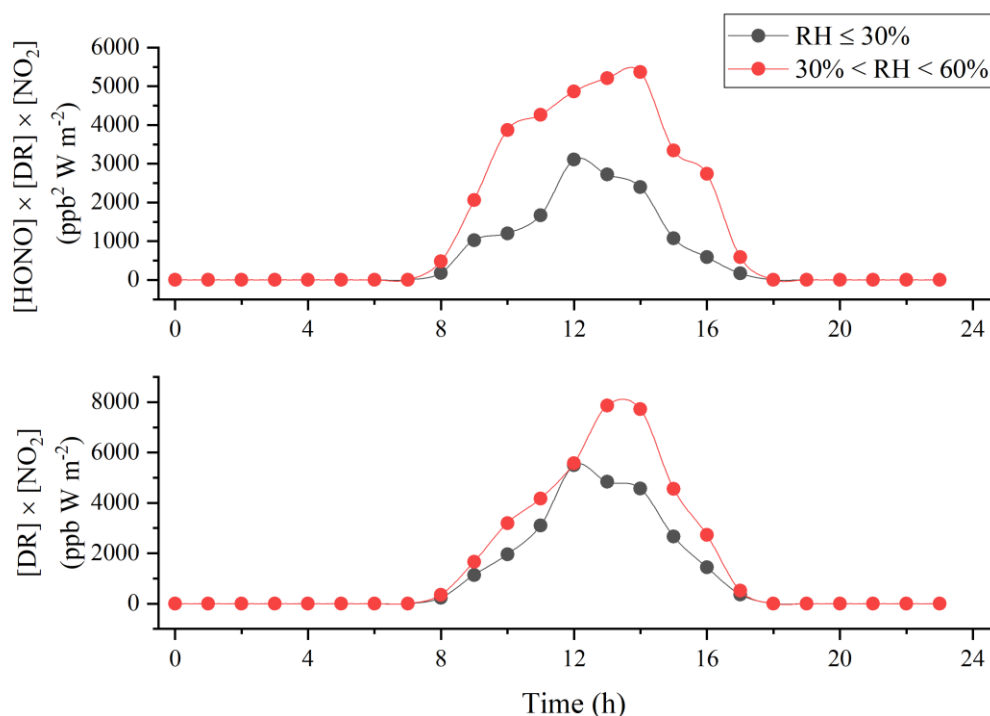
247 **Comment 6:** Though HONO is a main source OH, the diurnal variation of HONO may be different  
248 from OH radical. Have the author ever analyzed the correlation between  $\text{DR} \times \text{NO}_2$  and NOR?



249 Because the diurnal variation of OH radical should be highly correctly with radiation.

250

251 **Answer:** Because the photolysis of atmospheric HONO has been considered as the dominant OH  
252 source in polluted areas (Wang et al., 2017), the nitrate formation rate through the gas-phase reaction  
253 of NO<sub>2</sub> with OH radicals could be reflected by the product of [HONO] × [DR] × [NO<sub>2</sub>]. The evident  
254 difference for the diurnal variations between the products of [HONO] × [DR] × [NO<sub>2</sub>] and [DR] ×  
255 [NO<sub>2</sub>] implied that the relatively high HONO concentrations in the morning under the 30% < RH  
256 60% condition played a significant role in nitrate formation (Figure R6), which was in line with the  
257 variations of NOR (Figure 3 in the revised manuscript). Therefore, it may be more proper to use  
258 [HONO] × [DR] × [NO<sub>2</sub>] rather than [DR] × [NO<sub>2</sub>] for representing the gas-phase reaction of NO<sub>2</sub>  
259 with OH.



260

261 **Figure R6.** The comparison of the daily variations of [HONO] × [DR] × [NO<sub>2</sub>] and [DR] × [NO<sub>2</sub>]  
262 under the RH ≤ 30% condition and under the 30% < RH < 60% condition during the sampling  
263 period.

264

## 265 References

266 Gao, X., Yang, L., Cheng, S., Gao, R., Zhou, Y., Xue, L., Shou, Y., Wang, J., Wang, X., Nie, W.,  
267 Xu, P., and Wang, W.: Semi-continuous measurement of water-soluble ions in PM<sub>2.5</sub> in Jinan,  
268 China: Temporal variations and source apportionments, *Atmospheric Environment*, 45, 6048-6056,  
269 10.1016/j.atmosenv.2011.07.041, 2011.

270 Ponczek, M., Hayeck, N., Emmelin, C., and George, C.: Heterogeneous photochemistry of  
271 dicarboxylic acids on mineral dust, *Atmospheric Environment*, 212, 262-271,  
272 10.1016/j.atmosenv.2019.05.032, 2019.

273 Tang, M., Huang, X., Lu, K., Ge, M., Li, Y., Cheng, P., Zhu, T., Ding, A., Zhang, Y., Gligorovski,  
274 S., Song, W., Ding, X., Bi, X., and Wang, X.: Heterogeneous reactions of mineral dust aerosol:

275 implications for tropospheric oxidation capacity, *Atmospheric Chemistry and Physics*, 17, 11727-  
276 11777, 10.5194/acp-17-11727-2017, 2017.

277 Wang, J., Zhang, X., Guo, J., Wang, Z., and Zhang, M.: Observation of nitrous acid (HONO) in  
278 Beijing, China: Seasonal variation, nocturnal formation and daytime budget, *The Science of the*  
279 *total environment*, 587-588, 350-359, 10.1016/j.scitotenv.2017.02.159, 2017.

280 Zhang, R., Sun, X., Shi, A., Huang, Y., Yan, J., Nie, T., Yan, X., and Li, X.: Secondary inorganic  
281 aerosols formation during haze episodes at an urban site in Beijing, China, *Atmospheric*  
282 *Environment*, 177, 275-282, 10.1016/j.atmosenv.2017.12.031, 2018.

283 Zheng, G. J., Duan, F. K., Su, H., Ma, Y. L., Cheng, Y., Zheng, B., Zhang, Q., Huang, T., Kimoto,  
284 T., Chang, D., Pöschl, U., Cheng, Y. F., and He, K. B.: Exploring the severe winter haze in Beijing:  
285 the impact of synoptic weather, regional transport and heterogeneous reactions, *Atmospheric*  
286 *Chemistry and Physics*, 15, 2969-2983, 10.5194/acp-15-2969-2015, 2015.

287

A list of all relevant changes made in the manuscript

288

289 Based on the valuable comments and suggestions of the two reviewers, the followings are a list of  
290 all relevant changes made in the revised manuscript.

291

292 1. A brief description of NOR and SOR formulas has been added in abstract, and the NOR formula  
293 ( $\text{NOR} = \text{NO}_3^- / (\text{NO}_3^- + \text{NO}_2)$ ) rather than " $\text{NOR} = \text{NO}_3^- / (\text{NO}_3^- + \text{NO}_x)$ " has been corrected in our  
294 revised manuscript.

295 2. Solid evidences about the contribution of the heterogeneous hydrolysis of  $\text{N}_2\text{O}_5$  to the nocturnal  
296 formation of nitrate under the relatively high RH condition (the correlations and slopes between  
297 NOR and  $[\text{NO}_2]^2 \times [\text{O}_3]$ ) have been added in our revised manuscript.

298 3. The reason (the suppressed heterogeneous of  $\text{NO}_2$  rather than the deliquescence of nitrate) about  
299 the slow decrease of NOR under the  $\text{RH} \geq 60\%$  condition has been modified in our revised  
300 manuscript.

301 4. Figure 1 and Figure 3 have been amended for supporting the results and discussion in the  
302 manuscript.

303 5. the writing of the concentrations of species has been normalized by using square brackets in our  
304 revised manuscript.

305 6. Some logical and grammatical mistakes have been corrected in our revised manuscript.

306 7. Several references have been inserted to confirm our points in our revised manuscript.

307

308

309

310 Formation mechanisms of atmospheric nitrate and sulfate during the  
311 winter haze pollution periods in Beijing: gas-phase, heterogeneous  
312 and aqueous-phase chemistry

313 Pengfei Liu<sup>1, 2, 3, 5</sup>, Can Ye<sup>1, 3</sup>, Chaoyang Xue<sup>1, 3</sup>, Chenglong Zhang<sup>1, 2, 3</sup>, Yujing Mu<sup>1, 2, 3, 4</sup>, Xu  
314 Sun<sup>1, 6</sup>

315 <sup>1</sup> Research Center for Eco-Environmental Sciences, Chinese Academy of Sciences, Beijing, 100085, China.

316 <sup>2</sup> Center for Excellence in Urban Atmospheric Environment, Institute of Urban Environment, Chinese Academy of  
317 Sciences, Xiamen, 361021, China.

318 <sup>3</sup> University of Chinese Academy of Sciences, Beijing, 100049, China.

319 <sup>4</sup> National Engineering Laboratory for VOCs Pollution Control Material & Technology, University of Chinese  
320 Academy of Sciences, Beijing, 100049, China.

321 <sup>5</sup> Key Laboratory of Atmospheric Chemistry, China Meteorological Administration, Beijing, 100081, China.

322 <sup>6</sup> Beijing Urban Ecosystem Research Station, Beijing, 100085, China.

323 Correspondence: Yujing Mu ([yjmu@rcees.ac.cn](mailto:yjmu@rcees.ac.cn))

324 Abstract

325 A vast area in China is currently going through severe haze episodes with drastically elevated  
326 concentrations of PM<sub>2.5</sub> in winter. Nitrate and sulfate are main constituents of PM<sub>2.5</sub> but their  
327 formations via NO<sub>2</sub> and SO<sub>2</sub> oxidation are still not comprehensively understood, especially under  
328 different pollution or atmospheric relative humidity (RH) conditions. To elucidate formation  
329 pathways of nitrate and sulfate in different polluted cases, hourly samples of PM<sub>2.5</sub> were collected  
330 continuously in Beijing during the wintertime of 2016. Three serious pollution cases were identified  
331 reasonably during the sampling period and the secondary formations of nitrate and sulfate were  
332 found to make a dominant contribution to atmospheric PM<sub>2.5</sub> under the relatively high RH condition.

333 The significant correlation between NOR ( $NOR = NO_3^- / (NO_3^- + NO_2)$ ) and  $[NO_2]^2 \times [O_3]$  during the  
334 nighttime under the RH $\geq$ 60% condition indicated that the heterogeneous hydrolysis of N<sub>2</sub>O<sub>5</sub>  
335 involving aerosol liquid water was responsible for the nocturnal formation of nitrate at the extremely  
336 high RH levels. The more coincident trend of NOR and  $[HONO] \times [DR]$  (direct radiation)  $\times [NO_2]$

337 than  $\frac{[\text{Dust}] \times [\text{NO}_2]}{[\text{Dust}] \times [\text{NO}_2]}$  during the daytime under the 30%<RH<60% condition provided  
338 convincing evidence that the gas-phase reaction of NO<sub>2</sub> with OH played a pivotal role in the diurnal  
339 formation of nitrate at moderate RH levels. The extremely high mean values of SOR ( $\text{SOR} = \frac{\text{SO}_4^{2-}}{(\text{SO}_4^{2-} + \text{SO}_2)}$ )  
340  $\frac{(\text{SO}_4^{2-} + \text{SO}_2)}$  during the whole day under the RH≥60% condition could be ascribed to the evident  
341 contribution of SO<sub>2</sub> aqueous-phase oxidation to the formation of sulfate during the severe pollution  
342 episodes. Based on the parameters measured in this study and the known sulfate production rate  
343 calculation method, the oxidation pathway of H<sub>2</sub>O<sub>2</sub> rather than NO<sub>2</sub> was found to contribute greatly  
344 to the aqueous-phase formation of sulfate.

## 345 1. Introduction

346 In recent years, severe haze has occurred frequently in Beijing as well as the North China Plain  
347 (NCP) during the wintertime, which has aroused great attention from the public due to its adverse  
348 impact on atmospheric visibility, air quality and human health (Chan and Yao, 2008;Zhang et al.,  
349 2012;Zhang et al., 2015).

350 To mitigate the severe haze pollution situations, a series of regulatory measures for primary  
351 pollution sources have been implemented by the Chinese government. For example, coal  
352 combustion for heating in winter has gradually been replaced with electricity and natural gas in the  
353 NCP, coal-fired power plants have been strictly required to install flue-gas denitration and  
354 desulfurization systems (Chen et al., 2014), the stricter control measures such as terminating  
355 production in industries and construction as well as the odd and even number rule for vehicles have  
356 been performed in megacities during the period of the red alert for haze and so on. These actions  
357 have made tremendous effects to decline pollution levels of primary pollutants including PM<sub>2.5</sub> (fine  
358 particulate matter with an aerodynamic diameter less than 2.5 μm) in recent years (Li et al., 2019).

359 However, the serious pollution events still occurred in many areas of Beijing-Tianjin-Hebei (BTH)  
360 region in December 2016 and January 2017 (Li et al., 2019). It has been acknowledged that the  
361 severe haze pollution is mainly ascribed to stagnant meteorological conditions with high  
362 atmospheric relative humidity (RH) and low mixed boundary layer height, strong emissions of  
363 primary gaseous pollutants and rapid formation of secondary inorganic aerosols (SIAs, the sum of  
364 sulfate, nitrate and ammonium), especially sulfate and nitrate (Cheng et al., 2016;Guo et al.,  
365 2014;Huang et al., 2014). Some studies suggested that the contribution of SIAs to PM<sub>2.5</sub> was higher  
366 than 50% during the most serious haze days (Quan et al., 2014;Xu et al., 2017;Zheng et al., 2015a).

367 Generally, atmospheric sulfate and nitrate are formed through the oxidations of the precursor  
368 gases (SO<sub>2</sub> and NO<sub>2</sub>) by oxidants (e.g. OH radical, O<sub>3</sub>) via gas-phase, heterogeneous and aqueous-  
369 phase reactions (Ravishankara, 1997;Wang et al., 2013;Yang et al., 2015). It should be noted that  
370 the recent study proposed the remarkable emissions of primary sulfate from residential coal  
371 combustion with the sulfur contents of coal in range of 0.81-1.88% in Xi'an (Dai et al., 2019), but  
372 the primary emissions of sulfate could be neglected due to the extremely low sulfur content of coal  
373 (0.26-0.34%) used prevalingly in the NCP (Du et al., 2016;Li et al., 2016). Atmospheric RH is a  
374 key factor that facilitates the SIAs formation and aggravates the haze pollution (Wu et al., 2019),  
375 and hence the secondary formations of sulfate and nitrate are simply considered to be mainly via  
376 gas-phase reaction at relatively low atmospheric RH levels (RH<30%) and heterogeneous reactions  
377 and aqueous-phase reactions at relatively high atmospheric RH levels (RH>60%) (Li et al., 2017).  
378 However, their formation mechanisms at different atmospheric RH levels still remain controversial  
379 and unclear (Cheng et al., 2016;Ge et al., 2017;Guo et al., 2017;Li et al., 2018;Liu et al., 2017a;Wang  
380 et al., 2016;Yang et al., 2017). For example, the recent studies proposed that atmospheric SO<sub>2</sub>

381 oxidation by  $\text{NO}_2$  dissolved in aqueous aerosol phases under the extremely high atmospheric RH  
382 conditions played a dominant role in sulfate formation under almost neutral aerosol solutions (a pH  
383 range of 5.4-7.0) during the serious pollution periods (Cheng et al., 2016; Wang et al., 2018a; Wang  
384 et al., 2016). However, Liu et al. (2017a) and Guo et al. (2017) found that the aerosol pH estimated  
385 by ISORROPIA-II model was moderately acidic (a pH range of 3.0-4.9) and thus the pathway of  
386  $\text{SO}_2$  aqueous-phase oxidation by dissolved  $\text{NO}_2$  was unimportant during severe haze events in China.  
387 Additionally, although the pathway of  $\text{N}_2\text{O}_5$  heterogeneous hydrolysis has been recognized as being  
388 responsible for the nocturnal formation of  $\text{NO}_3^-$  under relatively high atmospheric RH conditions  
389 (Tham et al., 2018; Wang et al., 2018b; Wang et al., 2018c), the effects of  $\text{NO}_2$  gas-phase chemistry  
390 and  $\text{NO}_2$  heterogeneous chemistry on the diurnal formation of  $\text{NO}_3^-$  under moderate atmospheric  
391 RH conditions ( $30\% < \text{RH} < 60\%$ ) have not yet been understood. Therefore, measurements of the  
392 species in  $\text{PM}_{2.5}$  in different polluted cases during the wintertime are urgently needed to elucidate  
393 formation pathways of sulfate and nitrate.

394 In this study, hourly filter samples of  $\text{PM}_{2.5}$  were collected continuously in Beijing during the  
395 wintertime of 2016, and the pollution characteristics and formation mechanisms of sulfate and  
396 nitrate in the  $\text{PM}_{2.5}$  samples were investigated comprehensively under different atmospheric RH  
397 conditions in relation to gas-phase, heterogeneous and aqueous-phase chemistry.

## 398 **2. Materials and Methods**

### 399 **2.1. Sampling and analysis**

400 The sampling site was chosen on the rooftop (around 25 m above the ground) of a six-story  
401 building in Research Center for Eco-Environmental Sciences, Chinese Academy of Sciences  
402 (RCEES, CAS), which was located in the northwest of Beijing and had been described in detail by

403 our previous studies (Liu et al., 2016a;Liu et al., 2017b). The location of the sampling site  
404 (40°00'29.85" N, 116°20'29.71" E) is presented in Figure S1. Hourly PM<sub>2.5</sub> samples were collected  
405 on prebaked quartz fiber filters (90mm, Munktell) from January 7<sup>th</sup> to 23<sup>th</sup> of 2016 by median-  
406 volume samplers (Laoying-2030) with a flow rate of 100 L min<sup>-1</sup>. Water-soluble ions (WSI),  
407 including Na<sup>+</sup>, NH<sub>4</sub><sup>+</sup>, Mg<sup>2+</sup>, Ca<sup>2+</sup>, K<sup>+</sup>, Cl<sup>-</sup>, NO<sub>2</sub><sup>-</sup>, NO<sub>3</sub><sup>-</sup> and SO<sub>4</sub><sup>2-</sup>, as well as carbon components  
408 including organic carbon (OC) and element carbon (EC) in the filter samples were analyzed by ion  
409 chromatography (Wayeal IC6200) and thermal optical carbon analyzer (DRI-2001A), respectively  
410 (Liu et al., 2017b). Analysis relevant for quality assurance & quality control (QA/QC) was presented  
411 in detail in section M1 of the Supplementary Information (SIs). Atmospheric H<sub>2</sub>O<sub>2</sub> and HONO were  
412 monitored by AL2021-H<sub>2</sub>O<sub>2</sub> monitor (AERO laser, Germany) and a set of double-wall glass  
413 stripping coil sampler coupled with ion chromatography (SC-IC), respectively (Ye et al., 2018;Xue  
414 et al., 2019a;Xue et al., 2019b). More details about the measurements of H<sub>2</sub>O<sub>2</sub> and HONO were  
415 ascribed in section M2 of the SIs. Meteorological data, including wind speed, wind direction,  
416 ambient temperature and RH, as well as air quality index (AQI) derived by PM<sub>2.5</sub>, SO<sub>2</sub>, NO<sub>x</sub>, CO  
417 and O<sub>3</sub> were obtained from Beijing urban ecosystem research station in RCEES, CAS  
418 (<http://www.bjurban.rcees.cas.cn/>).

## 419 **2.2. Aerosol liquid water contents and pH prediction by ISORROPIA-II model**

420 The ISORROPIA-II model was employed to calculate the equilibrium composition for Na<sup>+</sup>-  
421 K<sup>+</sup>-Ca<sup>2+</sup>-Mg<sup>2+</sup>-NH<sub>4</sub><sup>+</sup>-Cl<sup>-</sup>-NO<sub>3</sub><sup>-</sup>-SO<sub>4</sub><sup>2-</sup>-H<sub>2</sub>O aerosol system, which is widely used in regional and  
422 global atmospheric models and has been successfully applied in numerous studies for predicting the  
423 physical state and composition of atmospheric inorganic aerosols (Fountoukis and Nenes, 2007;Guo  
424 et al., 2015;Shi et al., 2017). It can be used in two modes: forward mode and reverse mode. Forward



425 mode calculates the equilibrium partitioning given the total concentrations of gas and aerosol  
426 species, whereas reverse mode involves predicting the thermodynamic compositions based only on  
427 the concentrations of aerosol components. Forward mode was adopted in this study because reverse  
428 mode calculations have been verified to be not suitable to characterize aerosol acidity (Guo et al.,  
429 2015;Hennigan et al., 2015;Murphy et al., 2017;Pathak et al., 2004;Weber et al., 2016). The  
430 ISORROPIA-II model is available in “metastable” or “solid + liquid” state solutions. Considering  
431 the relatively high RH during the sampling period, the metastable state solution was selected in this  
432 study due to its better performance than the latter (Bougiatioti et al., 2016;Guo et al., 2015;Liu et  
433 al., 2017a;Weber et al., 2016). Additionally, although the gaseous HNO<sub>3</sub>, H<sub>2</sub>SO<sub>4</sub>, HCl and NH<sub>3</sub> were  
434 not measured in this study, gas-phase input with the exception of NH<sub>3</sub> has an insignificant impact  
435 on the aerosol liquid water contents (ALWC) and pH calculation due to the lower concentrations of  
436 HNO<sub>3</sub>, H<sub>2</sub>SO<sub>4</sub> and HCl than NH<sub>3</sub> in the atmosphere (Ding et al., 2019;Guo et al., 2017). Based on  
437 the long-term measurement in the winter of Beijing, an empirical equation between NO<sub>x</sub> and NH<sub>3</sub>  
438 concentrations was derived from the previous study (Meng et al., 2011), that is, NH<sub>3</sub> (ppb) = 0.34 ×  
439 NO<sub>x</sub> (ppb) + 0.63, which was employed for estimating the NH<sub>3</sub> concentration in this study. The  
440 predicted daily average concentrations of NH<sub>3</sub> varied from 3.3 μg m<sup>-3</sup> to 36.9 μg m<sup>-3</sup>, with a mean  
441 value of 16.6 μg m<sup>-3</sup> and a median value of 14.6 μg m<sup>-3</sup>, which were in line with those (7.6-38.1 μg  
442 m<sup>-3</sup>, 18.2 μg m<sup>-3</sup> and 16.2 μg m<sup>-3</sup> for the daily average concentrations, the mean value and the median  
443 value of NH<sub>3</sub>, respectively) during the winter of 2013 in Beijing in the previous study (Zhao et al.,  
444 2016).

445 Then, the aerosol pH could be calculated by the following equation:

446 
$$pH = -\log_{10} \frac{1000 \times H^+}{W}$$

447 where  $H^+$  ( $\mu\text{g m}^{-3}$ ) and  $W$  ( $\mu\text{g m}^{-3}$ ) are the equilibrium particle hydrogen ion concentration and  
 448 aerosol water contents, respectively, both of which could be output from ISORROPIA-II.

### 449 2.3. Production of sulfate in aqueous-phase reactions

450 The previous studies showed that there were six pathways of the aqueous-phase oxidation of  
 451  $\text{SO}_2$  to the production of sulfate, i.e.  $\text{H}_2\text{O}_2$  oxidation,  $\text{O}_3$  oxidation,  $\text{NO}_2$  oxidation, transition metal  
 452 ions (TMI) +  $\text{O}_2$  oxidation, methyl hydrogen peroxide (MHP) oxidation and peroxyacetic acid (PAA)  
 453 oxidation (Cheng et al., 2016;Zheng et al., 2015a). Because some TMIs, such as Ti(III), V(III),  
 454 Cr(III), Co(II), Ni(II), Cu(II) and Zn(II), displayed much less catalytic activities (Cheng et al., 2016),  
 455 only Fe(III) and Mn(II) were considered in this study. In addition, due to the extremely low  
 456 concentrations of MHP and PAA in the atmosphere, their contributions to the production of sulfate  
 457 could be ignored (Zheng et al., 2015a). To investigate the formation mechanism of sulfate during  
 458 the serious pollution episodes, the contributions of  $\text{O}_3$ ,  $\text{H}_2\text{O}_2$ ,  $\text{NO}_2$  and Fe(III) + Mn(II) to the  
 459 production of sulfate in aqueous-phase reactions were calculated by the formulas as follows (Cheng  
 460 et al., 2016;Ibusuki and Takeuchi, 1987;Seinfeld and Pandis, 2006):

$$461 \quad -\left(\frac{d[S(IV)]}{dt}\right)_{\text{O}_3} = (k_0[\text{SO}_2 \cdot \text{H}_2\text{O}] + k_1[\text{HSO}_3^-] + k_2[\text{SO}_3^{2-}])[\text{O}_3(\text{aq})] \quad (\text{R1})$$

$$462 \quad -\left(\frac{d[S(IV)]}{dt}\right)_{\text{H}_2\text{O}_2} = \frac{k_3[\text{H}^+][\text{HSO}_3^-][\text{H}_2\text{O}_2(\text{aq})]}{1+K[\text{H}^+]} \quad (\text{R2})$$

$$463 \quad -\left(\frac{d[S(IV)]}{dt}\right)_{\text{Fe(III)+Mn(II)}} = k_4[\text{H}^+]^a[\text{Mn(II)}][\text{Fe(III)}][\text{S(IV)}] \quad (\text{R3})$$

$$464 \quad -\left(\frac{d[S(IV)]}{dt}\right)_{\text{NO}_2} = k_5[\text{NO}_2(\text{aq})][\text{S(IV)}] \quad (\text{R4})$$

465 where  $k_0 = 2.4 \times 10^4 \text{ M}^{-1} \text{ s}^{-1}$ ,  $k_1 = 3.7 \times 10^5 \text{ M}^{-1} \text{ s}^{-1}$ ,  $k_2 = 1.5 \times 10^9 \text{ M}^{-1} \text{ s}^{-1}$ ,  $k_3 = 7.45 \times 10^7 \text{ M}^{-1} \text{ s}^{-1}$ ,  $K =$   
 466  $13 \text{ M}^{-1}$ ,  $k_4 = 3.72 \times 10^7 \text{ M}^{-1} \text{ s}^{-1}$ ,  $a = -0.74$  ( $\text{pH} \leq 4.2$ ) or  $k_4 = 2.51 \times 10^{13} \text{ M}^{-1} \text{ s}^{-1}$ ,  $a = 0.67$  ( $\text{pH} > 4.2$ ), and  
 467  $k_5 = (1.24-1.67) \times 10^7 \text{ M}^{-1} \text{ s}^{-1}$  ( $5.3 \leq \text{pH} \leq 8.7$ , the linear interpolated values were used for pH between  
 468 5.3 and 8.7) at 298 K (Clifton et al., 1988);  $[\text{O}_3(\text{aq})]$ ,  $[\text{H}_2\text{O}_2(\text{aq})]$  and  $[\text{NO}_2(\text{aq})]$  could be calculated by

469 the Henry's constants which are  $1.1 \times 10^{-2} \text{ M atm}^{-1}$ ,  $1.0 \times 10^5 \text{ M atm}^{-1}$  and  $1.0 \times 10^{-2} \text{ M atm}^{-1}$  at 298 K  
 470 for  $\text{O}_3$ ,  $\text{H}_2\text{O}_2$  and  $\text{NO}_2$  respectively (Seinfeld and Pandis, 2006). As for  $[\text{Fe(III)}]$  and  $[\text{Mn(II)}]$ , their  
 471 concentrations entirely depended on the values of pH due to the precipitation equilibriums of  
 472  $\text{Fe(OH)}_3$  and  $\text{Mn(OH)}_2$  (Graedel and Weschler, 1981). Considering the aqueous-phase ionization  
 473 equilibrium of  $\text{SO}_2$ , the Henry's constants of  $\text{HSO}_3^-$ ,  $\text{SO}_3^{2-}$  and  $\text{S(IV)}$  could be expressed by the  
 474 equations as follows (Seinfeld and Pandis, 2006):

$$475 \quad H_{\text{HSO}_3^-}^* = H_{\text{SO}_2} \frac{K_{\text{S1}}}{[\text{H}^+]} \quad (\text{R5})$$

$$476 \quad H_{\text{SO}_3^{2-}}^* = H_{\text{SO}_2} \frac{K_{\text{S1}}K_{\text{S2}}}{[\text{H}^+]^2} \quad (\text{R6})$$

$$477 \quad H_{\text{S(IV)}}^* = H_{\text{SO}_2} \left(1 + \frac{K_{\text{S1}}}{[\text{H}^+]} + \frac{K_{\text{S1}}K_{\text{S2}}}{[\text{H}^+]^2}\right) \quad (\text{R7})$$

478 where  $H_{\text{SO}_2} = 1.23 \text{ M atm}^{-1}$ ,  $K_{\text{S1}} = 1.3 \times 10^{-2} \text{ M}$  and  $K_{\text{S2}} = 6.6 \times 10^{-8} \text{ M}$  at 298 K. In addition, all  
 479 of rate constants (k), Henry's constants (H) and ionization constants (K) are evidently influenced on  
 480 the ambient temperature and are calibrated by the formulas as follows (Seinfeld and Pandis, 2006):

$$481 \quad k(T) = k(T_0) e^{\left[-\frac{E}{R} \left(\frac{1}{T} - \frac{1}{T_0}\right)\right]} \quad (\text{R8})$$

$$482 \quad H(T) = H(T_0) e^{\left[-\frac{\Delta H}{R} \left(\frac{1}{T} - \frac{1}{T_0}\right)\right]} \quad (\text{R9})$$

$$483 \quad K(T) = K(T_0) e^{\left[-\frac{E}{R} \left(\frac{1}{T} - \frac{1}{T_0}\right)\right]} \quad (\text{R10})$$

484 where T is the ambient temperature,  $T_0=298 \text{ K}$ , both  $E/R$  and  $\Delta H/R$  varied in the different  
 485 equations and their values could be found in Cheng et al., (2016).

486 Furthermore, mass transport was also considered for multiphase reactions in different medium  
 487 and across the interface in section M3 of the SIs.

### 488 3. Results and Discussion

#### 489 3.1. Variation characteristics of the species in $\text{PM}_{2.5}$ and typical gaseous pollutants

490 The concentrations of the species in  $\text{PM}_{2.5}$  and typical gaseous pollutants including  $\text{NO}_x$ ,  $\text{NO}_2$ ,

491 SO<sub>2</sub>, O<sub>3</sub>, HONO and H<sub>2</sub>O<sub>2</sub> as well as atmospheric RH are shown in Figure 1. The meteorological  
492 parameters (wind speed, wind direction, ambient temperature and direct radiation (DR)) as well as  
493 the concentrations of PM<sub>2.5</sub> are displayed in Figure S2. During the sampling period, the  
494 concentrations of the species in PM<sub>2.5</sub> and typical gaseous pollutants varied similarly on a timescale  
495 of hours with a distinct periodic cycle of 3-4 days, suggesting that meteorological conditions played  
496 a vital role in accumulation and dispersion of atmospheric pollutants (Xu et al., 2011;Zheng et al.,  
497 2015b). For example, the relatively high levels of PM<sub>2.5</sub> (>100 μg m<sup>-3</sup>) usually occurred under the  
498 relatively stable meteorological conditions with the low south wind speed (<2 m s<sup>-1</sup>) and the high  
499 RH (>60%) which favored the accumulation of pollutants. Besides meteorological conditions, the  
500 extremely high concentrations of the species in PM<sub>2.5</sub> might be mainly ascribed to strong emissions  
501 of primary pollutants and rapid formation of secondary aerosols during the wintertime in Beijing.

502 The average concentrations of the species in PM<sub>2.5</sub> and typical gaseous pollutants during clean  
503 or slightly polluted (C&SP) episodes (PM<sub>2.5</sub><75 μg m<sup>-3</sup>), during polluted or heavy polluted (P&HP)  
504 episodes (PM<sub>2.5</sub>≥75 μg m<sup>-3</sup>) and during the whole sampling period are illustrated in Table 1. It is  
505 evident that the average concentrations of NO<sub>3</sub><sup>-</sup>, SO<sub>4</sub><sup>2-</sup>, NH<sub>4</sub><sup>+</sup>, OC and EC during P&HP episodes  
506 were about a factor of 5.0, 4.1, 6.1, 3.6 and 3.2 greater than those during C&SP episodes,  
507 respectively, indicating that the formations of SIAs were more efficient compared to other species  
508 in PM<sub>2.5</sub> during the serious pollution episodes. Given that the average concentrations of gaseous  
509 precursors (NO<sub>2</sub> and SO<sub>2</sub>) during P&HP episodes were approximately a factor of 2.0-2.2 greater  
510 than those during C&SP episodes, the obviously higher elevation of NO<sub>3</sub><sup>-</sup> and SO<sub>4</sub><sup>2-</sup> implied that the  
511 oxidations of NO<sub>2</sub> and SO<sub>2</sub> by the major atmospheric oxidizing agents (OH radicals, O<sub>3</sub> and H<sub>2</sub>O<sub>2</sub>  
512 etc.) might be greatly accelerated due to the relatively high concentrations of oxidants and

513 atmospheric RH during the serious pollution episodes (Figure 1). The average concentration of H<sub>2</sub>O<sub>2</sub>  
514 was found to be a factor of 1.7 greater during P&HP episodes than during C&SP episodes, indicating  
515 that atmospheric H<sub>2</sub>O<sub>2</sub> might contribute to the formation of SIAs especially sulfate during the  
516 serious pollution episodes with high atmospheric RH, which will be discussed in Sect. 3.3.2.  
517 However, the obvious decrease in O<sub>3</sub> average concentration was observed during P&HP episodes  
518 compared to C&SP episodes, which was mainly attributed to the relatively weak solar radiation and  
519 the titration of NO during the serious pollution episodes (Ye et al., 2018). In addition, the evidently  
520 higher average concentration of HONO during P&HP episodes than during C&SP episodes might  
521 be also due to the relatively weak solar radiation as well as the heterogeneous reaction of NO<sub>2</sub> on  
522 particle surfaces during the serious pollution episodes (Tong et al., 2016; Wang et al., 2017).

### 523 **3.2. Three serious pollution cases during the sampling period**

524 Based on the transition from the clean to polluted periods, three haze cases were identified  
525 during the sampling period (Figure 1 and Figure S2): from 13:00 on January 8<sup>th</sup> to 1:00 on January  
526 11<sup>th</sup> (Case 1), from 14:00 on January 14<sup>th</sup> to 7:00 on January 17<sup>th</sup> (Case 2), and from 8:00 on January  
527 19<sup>th</sup> to 2:00 on January 22<sup>nd</sup> (Case 3). The serious pollution duration in the three cases could last 1-  
528 3 days due to the differences of their formation mechanisms.

529 In Case 1, the variation trends of the concentrations of the species in PM<sub>2.5</sub>, ~~NO<sub>x</sub>~~NO<sub>2</sub>, SO<sub>2</sub>,  
530 HONO and H<sub>2</sub>O<sub>2</sub> were almost identical and exhibited three pollution peaks at night (Figure 1),  
531 which might be ascribed to the possibility that the decrease of nocturnal mixed boundary layer  
532 accelerated the pollutant accumulation (Bei et al., 2017; Zhong et al., 2019). Considering the  
533 relatively low RH (15-40%) and wind speeds (<2 m s<sup>-1</sup>) in Case 1 (Figure S2), primary emissions  
534 around the sampling site were suspected to be a dominant source for the increase in the PM<sub>2.5</sub>

535 concentrations. Further evidence is that the correlation between the concentrations of PM<sub>2.5</sub> and CO  
536 is better in Case 1 ( $R^2=0.55$ ) than in Case 2 and Case 3 ( $R^2=0.20\sim0.52$ ) (Figure S3). Identical to  
537 Case 1, three obvious pollution peaks were also observed in Case 2 (Figure 1). The variation trends  
538 of the concentrations of the species in PM<sub>2.5</sub> and typical gaseous pollutants at the first peak in Case  
539 2 were found to be similar with those in Case 1, which were mainly attributed to their similar  
540 formation mechanism. However, the evident decreases in NO<sub>x</sub> and SO<sub>2</sub> were observed when the  
541 concentrations of the species in PM<sub>2.5</sub> were increasing and the atmospheric oxidation pollutant (e.g.  
542 H<sub>2</sub>O<sub>2</sub>) concentration peaks were prior to others at the last two peaks in Case 2, suggesting that  
543 secondary formation from gaseous precursors might be dominant for PM<sub>2.5</sub> pollution. The relatively  
544 high RH (50-80%) and the low south wind speeds (<2 m s<sup>-1</sup>) in Case 2 (Figure S2) provided further  
545 evidence for the above speculation. In contrast to Case 1 and Case 2, the relatively high south wind  
546 speeds (>3 m s<sup>-1</sup>) (Figure S2) with the concentrations of the species in PM<sub>2.5</sub> and typical gaseous  
547 pollutants increasing slowly (Figure 1) at the beginning of Case 3 indicated that regional  
548 transportation might be responsible for the atmospheric species. Subsequently, the concentrations  
549 of the species in PM<sub>2.5</sub> remained relatively high when the atmospheric RH lasted more than 60%,  
550 implying that secondary formation from gaseous precursors dominated PM<sub>2.5</sub> pollution during the  
551 late period of Case 3.

552 The average mass proportions of the species in PM<sub>2.5</sub> in the three cases are illustrated in Figure  
553 S4, the proportions of the primary species such as EC (10-13%), Cl<sup>-</sup> (6-7%) and Na<sup>+</sup> (4%) in the  
554 three cases were almost identical, indicating that primary particle emissions were relatively stable  
555 during the sampling period. However, the proportions of SIA in Case 2 (42%) and Case 3 (38%)  
556 were conspicuously greater than that in Case 1 (28%), further confirming that secondary formation

557 of inorganic ions (e.g. nitrate, sulfate) made a significant contribution to atmospheric PM<sub>2.5</sub> in Case  
558 2 and Case 3.

### 559 3.3. Formation mechanism of nitrate and sulfate during serious pollution episodes

560 As for nitrate and sulfate in the three cases, the highest mass proportion (18%) of nitrate was  
561 observed in Case 2, whereas the highest mass proportion (15%) of sulfate was found in Case 3  
562 (Figure S4). Although the concentrations of SO<sub>2</sub> were ~~about a factor of 5~~ obviously lower than the  
563 concentrations of NO<sub>2</sub> in both Case 2 and Case 3 (Figure 1 and Table 1), the extremely high  
564 proportion of sulfate in Case 3 might be ascribed to the long-lasting plateau of RH (Figure S2)  
565 because the aqueous-phase reaction could accelerate the conversion of SO<sub>2</sub> to SO<sub>4</sub><sup>2-</sup>. To further  
566 investigate the pollution characteristics of nitrate and sulfate during the serious pollution episodes,  
567 the relations between NOR (NOR = NO<sub>3</sub><sup>-</sup> / (NO<sub>3</sub><sup>-</sup>+NO<sub>x2</sub>)) as well as SOR (SOR = SO<sub>4</sub><sup>2-</sup> / (SO<sub>4</sub><sup>2-</sup>  
568 +SO<sub>2</sub>)) and RH are shown in Figure 2. There were obvious differences in the variations of NOR and  
569 SOR under different atmospheric RH conditions. The variation trends of NOR and SOR almost  
570 stayed the same when atmospheric RH was below 30%, and then simultaneously increased with  
571 atmospheric RH in the range of 30-60%. The enhanced gas-phase reaction and the heterogeneous  
572 reaction involving aerosol liquid water might make a remarkable contribution to the elevation of  
573 NOR and SOR, respectively, which were further discussed in the following section. Subsequently,  
574 the variation trend of NOR slowly decreased whereas the variation trend of SOR significantly  
575 increased when atmospheric RH was above 60%, which was very similar with the previous studies  
576 (Sun et al., 2013;Zheng et al., 2015b). Considering that the heterogeneous reactions of NO<sub>2</sub> on  
577 particle surface were dependent on atmospheric RH due to the competition of water for surface  
578 reactive sites of particles (Ponczek et al., 2019), tThe slow reduction of NOR might be due to the

579 ~~suppressed heterogeneous reaction of NO<sub>2</sub> to nitrate formation deliquescence of nitrate at~~  
580 ~~atmospheric under high RH condition around 60% (Tang et al., 2017)(Kuang et al., 2016;Liu et al.,~~  
581 ~~2016b;Xue et al., 2014)~~, while the elevation of SOR revealed the dominant contribution of the  
582 aqueous-phase reaction to ~~the sulfate formation of sulfate.~~

### 583 3.3.1. Formation mechanism of nitrate

584 Atmospheric nitrate is considered to be mainly from NO<sub>2</sub> oxidation by OH radical in the gas  
585 phase, heterogeneous uptake of NO<sub>2</sub> on the surface of particles and heterogeneous hydrolysis of  
586 N<sub>2</sub>O<sub>5</sub> on wet aerosols or chloride-containing aerosols (He et al., 2014;He et al., 2018;Nie et al.,  
587 2014;Ravishankara, 1997;Wang et al., 2018b). Since atmospheric N<sub>2</sub>O<sub>5</sub> is usually produced by the  
588 reaction of NO<sub>3</sub> radical with NO<sub>2</sub> as well as both NO<sub>3</sub> radical and N<sub>2</sub>O<sub>5</sub> are easily photolytic during  
589 the daytime, the heterogeneous hydrolysis of N<sub>2</sub>O<sub>5</sub> is a nighttime pathway for the formation of  
590 atmospheric nitrate (He et al., 2018;Wang et al., 2018b). As shown in Figure 3a, the mean values of  
591 NOR during the nighttime remarkably elevated with atmospheric RH increasing, the  
592 disproportionation of NO<sub>2</sub> and the heterogeneous hydrolysis of N<sub>2</sub>O<sub>5</sub> involving aerosol liquid water  
593 were suspected to dominate the nocturnal formation of nitrate under high RH conditions during the  
594 sampling period (Ma et al., 2017;Wang et al., 2018b;Li et al., 2018). However, the productions of  
595 HONO and nitrate should be equal through the disproportionation of NO<sub>2</sub> (Ma et al., 2017), which  
596 could not explain the wide gaps between the average concentrations of HONO (about 6.5 μg m<sup>-3</sup>)  
597 and nitrate (about 20.1 μg m<sup>-3</sup>) observed at the nighttime under high RH conditions during the  
598 sampling period. Thus, the disproportionation of NO<sub>2</sub> made insignificant contribution to the  
599 nocturnal formation of nitrate under high RH conditions. Considering that the formation of  
600 atmospheric NO<sub>3</sub> radical is mainly via the oxidation of NO<sub>2</sub> by O<sub>3</sub>, the heterogeneous hydrolysis of



601  $\text{N}_2\text{O}_5$  occurs only at high  $\text{O}_3$  and  $\text{NO}_2$  levels during the nighttime (He et al., 2018; Wang et al., 2018b).

602 Therefore, the correlation between  $[\text{NO}_2]^2 \times [\text{O}_3]$  and NOR can represent roughly the contribution

603 of the heterogeneous hydrolysis of  $\text{N}_2\text{O}_5$  to atmospheric nitrate at night. As shown in Figure 3b, the

604 variations of  $[\text{NO}_2]^2 \times [\text{O}_3]$  at the nighttime (18:00-7:00) were all positively correlated with NOR

605 under the three different RH conditions, and their correlation under the  $\text{RH} \geq 60\%$  condition ( $R^2 =$

606 0.552) was significantly stronger than those under the  $\text{RH} < 60\%$  condition ( $R^2 \leq 0.181$ ). It has been

607 acknowledged that the correlation between two species means the impact of changes in one species

608 on another. The stronger the correlation is, the greater the impact is. Therefore, the positive

609 correlations between NOR and  $[\text{NO}_2]^2 \times [\text{O}_3]$  indicated that the heterogeneous hydrolysis of  $\text{N}_2\text{O}_5$

610 could contribute to the formation of atmospheric nitrate at the nighttime under different RH

611 conditions. The significantly stronger correlations between NOR and  $[\text{NO}_2]^2 \times [\text{O}_3]$  under the RH

612  $\geq 60\%$  condition than under the  $\text{RH} < 60\%$  condition revealed that the heterogeneous hydrolysis of

613  $\text{N}_2\text{O}_5$  made a remarkable contribution to atmospheric nitrate at the nighttime under high RH

614 condition. Additionally, the obviously lower slope of the correlation between NOR and  $[\text{NO}_2]^2 \times$

615  $[\text{O}_3]$  under the  $\text{RH} \geq 60\%$  condition (slope = 11691) than under the  $\text{RH} < 60\%$  condition (slope  $\geq$

616 17399) (Figure 3b) also suggested that the formation of atmospheric nitrate at the nighttime under

617 high RH condition was more sensitive to the pathway of  $\text{N}_2\text{O}_5$ . the more significant correlation

618 between  $\text{NO}_2 \times \text{O}_3$  and NOR under the  $\text{RH} \geq 60\%$  condition ( $R^2 = 0.534$ ) than under the  $\text{RH} < 60\%$

619 condition ( $R^2 < 0.005$ ) at the nighttime (19:00-6:00) during the sampling period further confirmed

620 that the heterogeneous hydrolysis of  $\text{N}_2\text{O}_5$  on wet aerosols made a great contribution to atmospheric

621 nocturnal nitrate under high RH conditions.

622 However, the obvious increase in the mean values of NOR during the daytime (especially for

623 10:00-17:00) under the 30%<RH<60% condition (Figure 3a) indicated that additional sources rather  
624 than the heterogeneous hydrolysis of N<sub>2</sub>O<sub>5</sub> were responsible for the formation of nitrate. To explore  
625 the possible formation mechanisms of nitrate in this case, the daily variations of [Dust] (the sum of  
626 Ca<sup>2+</sup> and Mg<sup>2+</sup>) × [NO<sub>2</sub>] and [HONO] (the main source of OH) × [DR] × [NO<sub>2</sub>], which can represent  
627 roughly the heterogeneous reaction of NO<sub>2</sub> on the surface of mineral aerosols and the gas-phase  
628 reaction of NO<sub>2</sub> with OH, are shown in Figure 3c and Figure 3d, respectively. The mean values of  
629 ~~[HONO] × [DR] × [NO<sub>2</sub>]~~ during the daytime were found to be remarkably  
630 greater under the 30%<RH<60% condition than under the RH≤30% condition, whereas the mean  
631 values of ~~[Dust] × [NO<sub>2</sub>]~~ almost stayed the same under the two different RH conditions.  
632 Considering the coincident trend of NOR and ~~[HONO] × [DR] × [NO<sub>2</sub>]~~ during  
633 the daytime (10:00-17:00) under the 30%<RH<60% condition, the gas-phase reaction of NO<sub>2</sub> with  
634 OH played a key role in the diurnal formation of nitrate at moderate RH levels with the haze  
635 pollution accumulating. It should be noted that the mean values of ~~[HONO] × [DR] × [NO<sub>2</sub>]~~  
636 ~~× DR × NO<sub>2</sub>~~ decreased dramatically from 14:00 to 17:00 (Figure 3d), which was not responsible for  
637 the high mean values of NOR at that time (Figure 3a). However, the slight increase in the mean  
638 values of ~~[Dust] × [NO<sub>2</sub>]~~ after 14:00 was observed under the 30%<RH<60% condition  
639 (Figure 3c) and hence the heterogeneous reaction of NO<sub>2</sub> on the surface of mineral aerosols was  
640 suspected to contribute to the diurnal formation of nitrate at that time under moderate RH condition.

### 641 3.3.2. Formation mechanism of sulfate

642 Atmospheric sulfate is principally from SO<sub>2</sub> oxidation pathway, including gas-phase reactions  
643 with OH radical or stabilized Criegee intermediates, heterogeneous-phase reactions on the surface  
644 of particles and aqueous-phase reactions with dissolved O<sub>3</sub>, NO<sub>2</sub>, H<sub>2</sub>O<sub>2</sub> and organic peroxides, as

645 well as autoxidation catalyzed by TMI (Cheng et al., 2016;Li et al., 2018;Ravishankara, 1997;Shao  
646 et al., 2019;Wang et al., 2016;Xue et al., 2016;Zhang et al., 2018). As shown in Figure 4, similar to  
647 the daily variations of NOR, ~~the remarkable elevation of~~ the mean values of SOR were found to  
648 elevated remarkably after 14:00 under the  $30% < RH < 60%$  condition compared to the  $RH \leq 30%$   
649 condition, especially during 14:00-22:00, which might be ~~also mainly~~ ascribed to the enhanced gas-  
650 phase reaction and the heterogeneous reaction of  $SO_2$  involving aerosol liquid water on the surface  
651 of mineral aerosols under the relatively high RH condition. The extremely high mean values of SOR  
652 during the whole day under the  $RH \geq 60%$  condition implied that aqueous oxidation of  $SO_2$   
653 dominated the formation of sulfate during the severe pollution episodes, which was in line with  
654 previous studies (Zhang et al., 2018;Cheng et al., 2016). A key factor that influenced the aqueous  
655 oxidation pathways for sulfate formation has been considered to be the aerosol pH (Guo et al.,  
656 2017;Liu et al., 2017a), varying from 4.5 to 8.5 at different atmospheric RH and sulfate levels during  
657 the sampling period (Figure 5a) on the basis of the ISORROPIA-II model. Considering that the  
658 aqueous-phase chemistry of sulfate formation usually occurs in severe haze events with relatively  
659 high atmospheric RH, the aerosol pH (4.5-5.3) under the  $RH \geq 60%$  condition, which was lower than  
660 those (5.4-7.0) in the studies of Wang et al., (2016) and Cheng et al., (2016) but was slightly higher  
661 than those (3.0-4.9) in the studies of Liu et al., (2017a) and Guo et al., (2017), was adopted for  
662 evaluating sulfate production in this study. In addition, in terms of oxidants, the obvious increase in  
663 the average concentration of  $NO_2$  (Figure 5b) and the evident decrease in the average concentration  
664 of  $O_3$  (Figure 5d) were observed with the deterioration of  $PM_{2.5}$  pollution. Furthermore, the average  
665 concentration of  $H_2O_2$  was also found to be extremely high (0.25 ppb) under the HP condition  
666 (Figure 5c) and was above 1 order of magnitude higher than that (0.01 ppb) assumed by Cheng et

667 al., (2016), which probably resulted in the underestimation of the contribution of H<sub>2</sub>O<sub>2</sub> to sulfate  
668 formation in the study of Cheng et al., (2016).

669 To further explore the contribution of H<sub>2</sub>O<sub>2</sub> to sulfate production rate under the HP condition,  
670 the parameters measured in this study (Table 2) and the same approach that was adopted by Cheng  
671 et al., (2016) were used to calculate sulfate production. As shown in Figure 6, the relationships  
672 between different aqueous oxidation pathways and aerosol pH in this study were found to be very  
673 similar with those of Cheng et al., (2016). However, the contribution of H<sub>2</sub>O<sub>2</sub> to sulfate production  
674 rate was about a factor of 17 faster in this study (about 1.16 μg m<sup>-3</sup> h<sup>-1</sup>) than in the study (about  
675 6.95×10<sup>-2</sup> μg m<sup>-3</sup> h<sup>-1</sup>) of Cheng et al., (2016), implying that the contribution of H<sub>2</sub>O<sub>2</sub> to sulfate  
676 formation was largely neglected. Furthermore, considering the aerosol pH calculated under the HP  
677 condition during the sampling period, the oxidation pathway of NO<sub>2</sub> might play an insignificant role  
678 in sulfate production rate (8.96×10<sup>-2</sup>-0.56 μg m<sup>-3</sup> h<sup>-1</sup>) and its importance proposed by the previous  
679 studies (1.74-10.85 μg m<sup>-3</sup> h<sup>-1</sup>) was not necessarily expected.

#### 680 4. Conclusion

681 Based on the comprehensive analysis of the pollution levels, the variation characteristics and  
682 the formation mechanisms of the key species in PM<sub>2.5</sub> and the typical gaseous pollutants during the  
683 winter haze pollution periods in Beijing, three serious haze pollution cases were obtained during the  
684 sampling period and the SIAs formations especially nitrate and sulfate were found to make an  
685 evident contribution to atmospheric PM<sub>2.5</sub> under the relatively high RH condition. The significant  
686 correlation between  $[\text{NO}_2]^2 \times [\text{O}_3]$  and NOR at night under the RH≥60% condition indicated that  
687 the heterogeneous hydrolysis of N<sub>2</sub>O<sub>5</sub> on wet aerosols was responsible for the nocturnal formation  
688 of nitrate under extremely high RH conditions. The more coincident trend of NOR and  $[\text{HONO}] \times$

689  $[DR] \times [NO_2]HONO \times DR \times NO_2$  than  $[Dust] \times [NO_2]Dust \times NO_2$  during the daytime under the  
690 30%<RH<60% condition suggested that the gas-phase reaction of NO<sub>2</sub> with OH played a key role  
691 in the diurnal formation of nitrate under moderate RH conditions. The extremely high mean values  
692 of SOR during the whole day under the RH≥60% condition could be explained by the dominant  
693 contribution of aqueous-phase reaction of SO<sub>2</sub> to atmospheric sulfate formation during the severe  
694 pollution episodes. According to the parameters measured in this study and the same approach that  
695 was adopted by Cheng et al., (2016), the oxidation pathway of H<sub>2</sub>O<sub>2</sub> rather than NO<sub>2</sub> was found to  
696 contribute greatly to atmospheric sulfate formation.

697 Our results revealed that the heavy pollution events in winter usually occurred with high  
698 concentration levels of pollutants and oxidants as well as high liquid water contents of moderately  
699 acidic aerosols in the NCP. Thus, emission controls of NO<sub>x</sub>, SO<sub>2</sub> and VOCs especially under the  
700 extremely high RH conditions are expected to reduce largely the pollution levels of nitrate and  
701 sulfate in northern China and even in other pollution regions of China.

702

703 *Data availability.* Data are available from the corresponding author upon request  
704 ([yjmu@rcees.ac.cn](mailto:yjmu@rcees.ac.cn))

705

706 *Author contributions.* YJM designed the experiments. PFL carried out the experiments and prepared  
707 the manuscript. CY and CYX carried out the experiments. CLZ was involved in part of the work.  
708 XS provided the meteorological data and trace gases in Beijing.

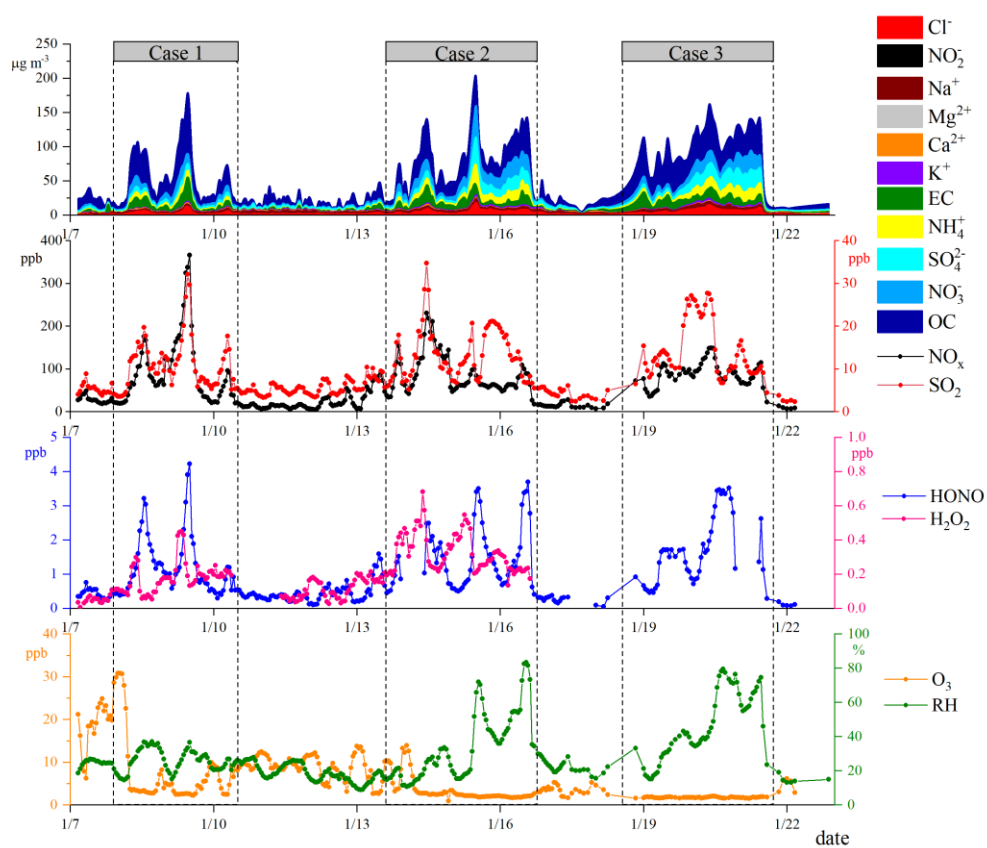
709

710 *Competing interests.* The authors declare that they have no conflict of interest.

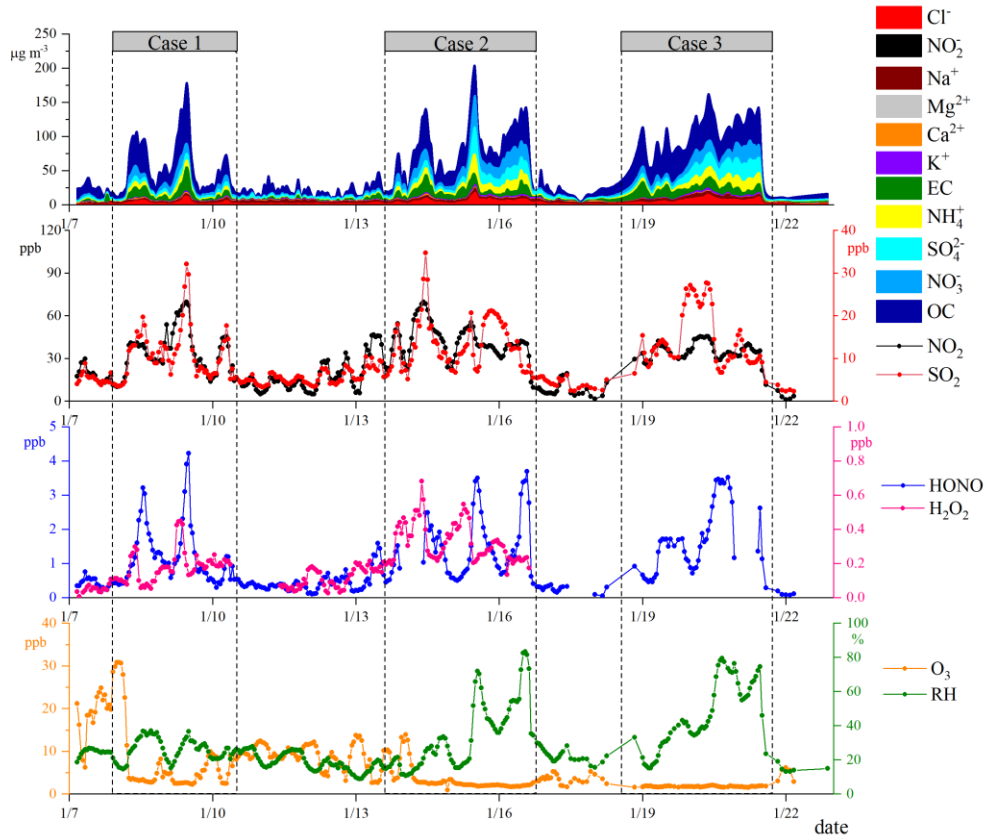
711

712 *Acknowledgement.* This work was supported by the National research program for Key issues in air  
713 pollution control (No. DQGG0103, DQGG0209, DQGG0206), the National Natural Science  
714 Foundation of China (No. 91544211, 4127805, 41575121, 21707151), the National Key Research  
715 and Development Program of China (No. 2016YFC0202200, 2017YFC0209703, 2017YFF0108301)  
716 and Key Laboratory of Atmospheric Chemistry, China Meteorological Administration (No.  
717 2018B03).

718



719



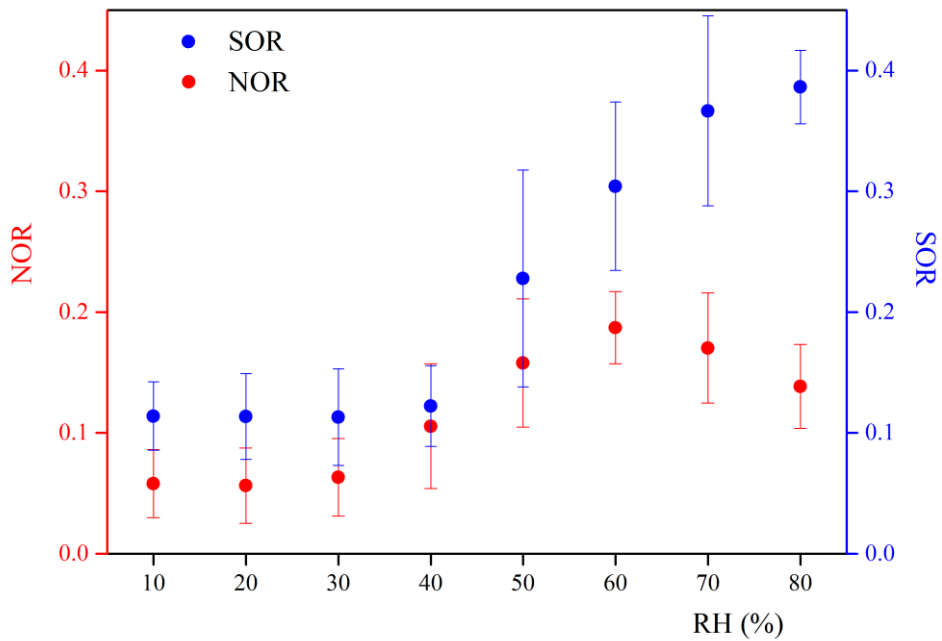
720

721

**Figure 1.** Time series of the species in PM<sub>2.5</sub> and typical gaseous pollutants ( $\text{NO}_x$ ,  $\text{NO}_2$ ,  $\text{SO}_2$ ,  $\text{O}_3$ , HONO and  $\text{H}_2\text{O}_2$ ) as well as atmospheric RH during the sampling period.

722

723



724

725

**Figure 2.** The relations between NOR as well as SOR and RH during the sampling period.

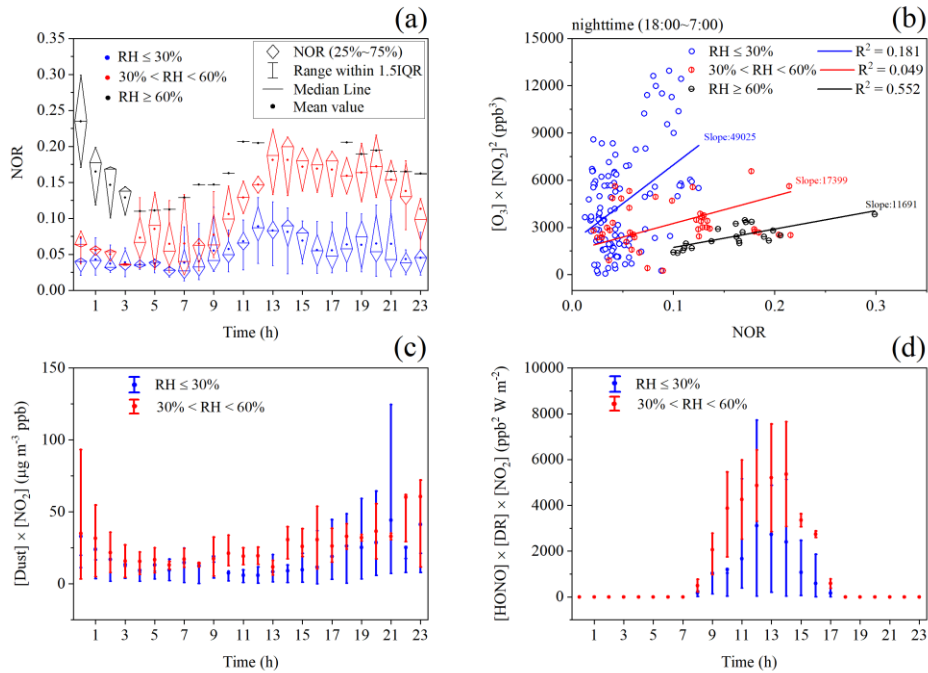
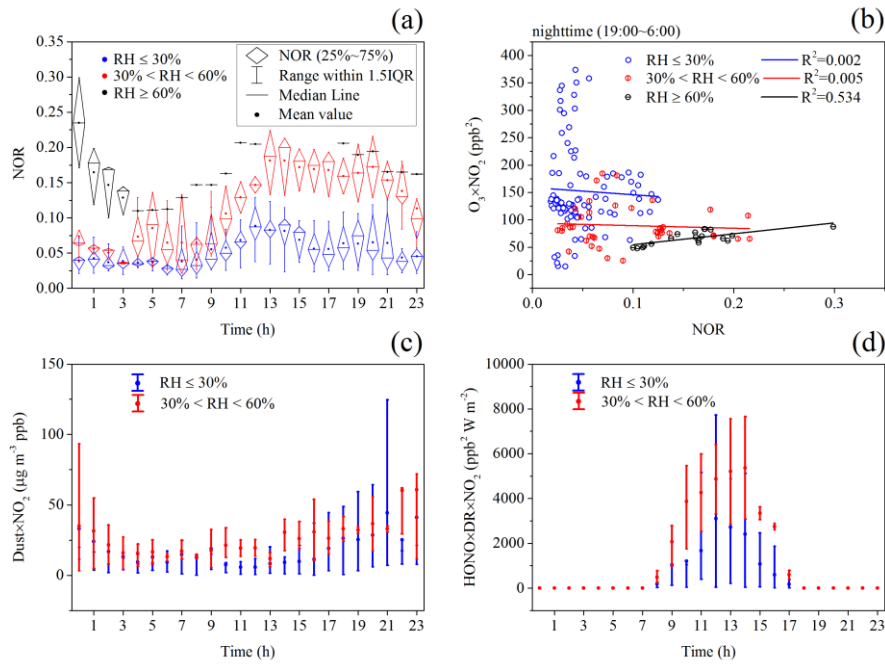
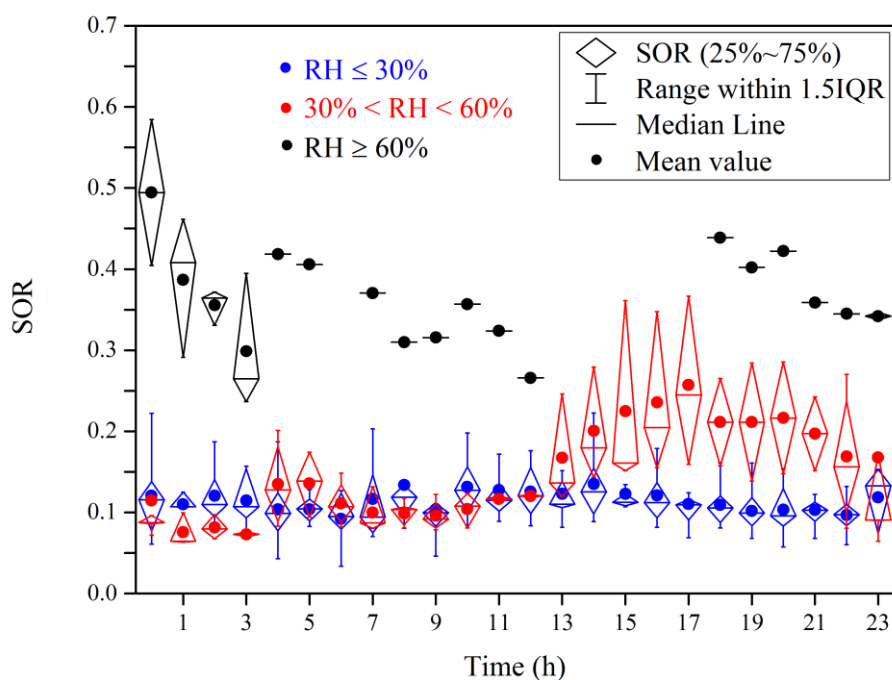


**Figure 3.** Daily variation of NOR (a), the correlation between NOR and  $[NO_2]^2 \times [O_3] \times NO_2$  at the nighttime (18:00-7:00) (b), daily variations of  $[Dust] \times [NO_2]$  and  $[HONO] \times [DR] \times [NO_2]$  (c, d) under different atmospheric RH conditions during the sampling period.





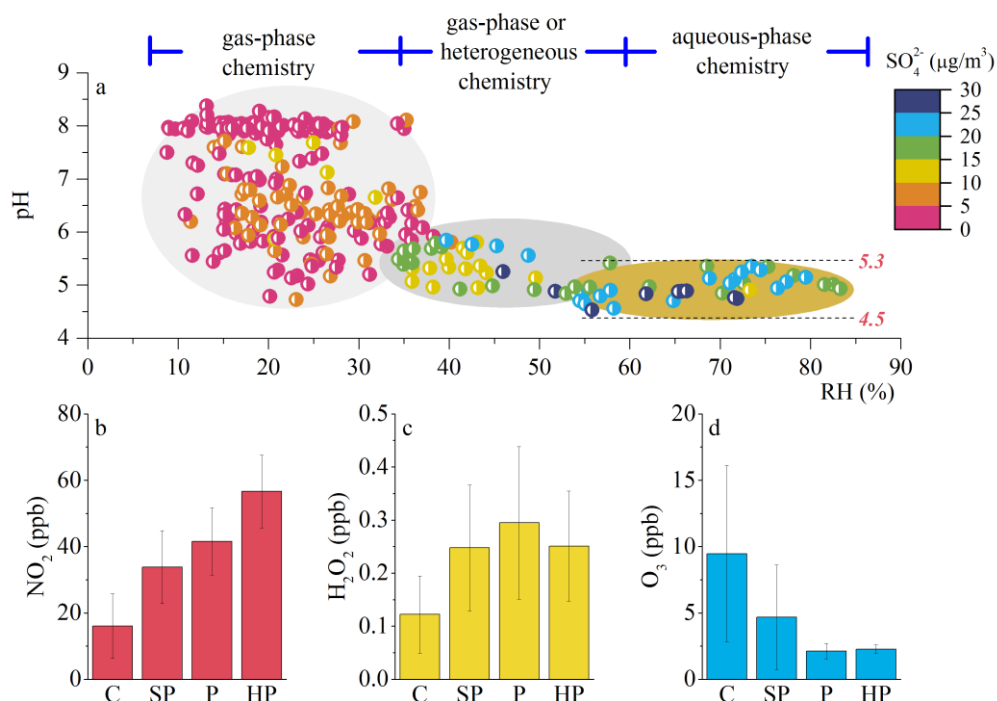
733

734

**Figure 4.** Daily variation of SOR under different atmospheric RH conditions during the sampling period.

735

736



737

738

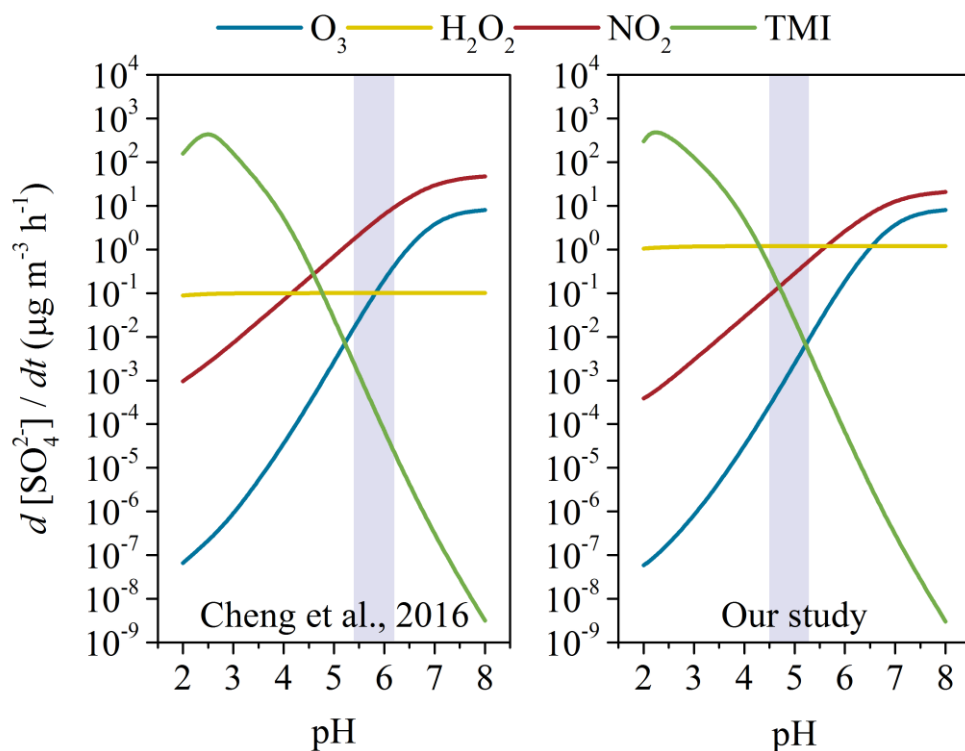
739

740

**Figure 5.** The correlations among aerosol pH, atmospheric RH and atmospheric  $\text{SO}_4^{2-}$  (a), the average concentrations of  $\text{NO}_2$ ,  $\text{H}_2\text{O}_2$  and  $\text{O}_3$  (b, c, d) under different pollution conditions (clean (C),  $\text{PM}_{2.5} < 35 \mu\text{g m}^{-3}$ ; slightly polluted (SP),  $35 \mu\text{g m}^{-3} < \text{PM}_{2.5} < 75 \mu\text{g m}^{-3}$ ; polluted (P),  $75 \mu\text{g m}^{-3} < \text{PM}_{2.5} < 150 \mu\text{g m}^{-3}$ ; heavily polluted (HP),  $\text{PM}_{2.5} > 150 \mu\text{g m}^{-3}$ ).

741  
742

$^{3}<PM_{2.5}<150 \mu g m^{-3}$ ; heavy polluted (HP),  $PM_{2.5}>150 \mu g m^{-3}$ ) during the sampling period.



743  
744  
745  
746  
747  
748  
749

**Figure 6.** The comparison of aqueous-phase sulfate production by  $SO_2$  oxidation under different aerosol pH conditions between in the study of Cheng et al., (2016) and in this study.

**Table 1.** The average concentrations of the species in  $PM_{2.5}$  ( $\mu g m^{-3}$ ) and typical gaseous pollutants (ppb) during C&SP episodes ( $PM_{2.5}<75 \mu g m^{-3}$ ), during P&HP episodes ( $PM_{2.5}\geq 75 \mu g m^{-3}$ ) and during the whole sampling period.

species	during C&SP episodes (n=210)	during P&HP episodes (n=108)	total (n=318)
$PM_{2.5}$	$30.00 \pm 17.79$	$113.35 \pm 28.10$	$58.31 \pm 45.15$
$Na^+$	$2.88 \pm 1.11$	$3.68 \pm 1.19$	$3.15 \pm 1.21$
$Mg^{2+}$	$0.05 \pm 0.03$	$0.08 \pm 0.06$	$0.06 \pm 0.04$
$Ca^{2+}$	$0.52 \pm 0.33$	$0.67 \pm 0.48$	$0.58 \pm 0.40$
$K^+$	$0.81 \pm 0.42$	$1.84 \pm 0.73$	$1.16 \pm 0.73$
$NH_4^+$	$1.90 \pm 1.90$	$11.52 \pm 4.93$	$5.17 \pm 5.62$
$SO_4^{2-}$	$3.64 \pm 1.87$	$14.96 \pm 7.80$	$7.47 \pm 7.18$
$NO_3^-$	$3.44 \pm 3.57$	$17.15 \pm 7.36$	$8.10 \pm 8.32$
$Cl^-$	$1.89 \pm 1.20$	$7.35 \pm 2.97$	$3.73 \pm 3.26$
$NO_2^-$	$0.06 \pm 0.08$	$0.06 \pm 0.05$	$0.06 \pm 0.07$
OC	$12.10 \pm 9.25$	$43.34 \pm 13.88$	$22.73 \pm 18.48$
EC	$3.98 \pm 3.42$	$12.69 \pm 6.43$	$7.58 \pm 6.51$
$NO_x$	$39.38 \pm 35.25$	$107.71 \pm 58.44$	$62.59 \pm 54.98$
$NO_2$	$21.46 \pm 13.04$	$42.81 \pm 10.96$	$28.71 \pm 15.98$
$SO_2$	$6.99 \pm 3.64$	$15.70 \pm 6.55$	$9.95 \pm 6.35$

O <sub>3</sub>	8.01 ± 6.35	2.13 ± 0.56	6.01 ± 5.87
HONO	0.60 ± 0.43	1.90 ± 0.97	1.01 ± 0.87
H <sub>2</sub> O <sub>2</sub>	0.17 ± 0.11	0.29 ± 0.14	0.20 ± 0.13

750

751

752

**Table 2.** The comparisons for parameters of sulfate production rate calculations between in the study of Cheng et al., (2016) and in this work during the most polluted haze periods

Parameters	This study	Cheng et al., (2016)
NO <sub>2</sub>	57 ppb	66 ppb
H <sub>2</sub> O <sub>2</sub>	0.25 ppb	0.01 ppb
O <sub>3</sub>	2 ppb	1 ppb
SO <sub>2</sub>	35 ppb	40 ppb
Fe(III) <sup>a</sup>	18 ng m <sup>-3</sup>	18 ng m <sup>-3</sup>
Mn(II) <sup>a</sup>	42 ng m <sup>-3</sup>	42 ng m <sup>-3</sup>
ALWC	146 µg m <sup>-3</sup>	300 µg m <sup>-3</sup>
Aerosol droplet radius (R) <sup>a</sup>	0.15 µm	0.15 µm
Temperature	270 K	271 K
pH	4.5-5.3	5.4-6.2

753

<sup>a</sup>: both the concentrations of Fe(III) and Mn(II) and aerosol droplet radius were not measured in this study and were derived from Cheng et al., (2016).

754

755

756

## References

757

Bei, N., Wu, J., Elser, M., Feng, T., Cao, J., El-Haddad, I., Li, X., Huang, R., Li, Z., Long, X., Xing, L., Zhao, S., Tie, X., Prévôt, A. S. H., and Li, G.: Impacts of meteorological uncertainties on the haze formation in Beijing–Tianjin–Hebei (BTH) during wintertime: a case study, *Atmospheric Chemistry and Physics*, 17, 14579-14591, 10.5194/acp-17-14579-2017, 2017.

761

Bougiatioti, A., Nikolaou, P., Stavroulas, I., Kouvarakis, G., Weber, R., Nenes, A., Kanakidou, M., and Mihalopoulos, N.: Particle water and pH in the eastern Mediterranean: source variability and implications for nutrient availability, *Atmospheric Chemistry and Physics*, 16, 4579-4591, 10.5194/acp-16-4579-2016, 2016.

765

Chan, C. K., and Yao, X.: Air pollution in mega cities in China, *Atmospheric Environment*, 42, 1-42, 10.1016/j.atmosenv.2007.09.003, 2008.

767

Chen, L. H., Sun, Y. Y., Wu, X. C., Zhang, Y. X., Zheng, C. H., Gao, X., and Cen, K.: Unit-based emission inventory and uncertainty assessment of coal-fired power plants, *Atmospheric Environment*, 99, 527-535, 10.1016/j.atmosenv.2014.10.023, 2014.

770

Cheng, Y., Zheng, G., Wei, C., Mu, Q., Zheng, B., Wang, Z., Gao, M., Zhang, Q., He, K., Carmichael, G., Pöschl, U., and Su, H.: Reactive nitrogen chemistry in aerosol water as a source of sulfate during haze events in China, *Science Advances*, 2, 1-11, 10.1126/sciadv.1601530, 2016.

773

Clifton, C. L., Altstein, N., and Huie, R. E.: Rate-constant for the reaction of NO<sub>2</sub> with sulfur(IV) over the pH range 5.3-13, *Environ. Sci. Technol.*, 22, 586-589, 10.1021/es00170a018, 1988.

775

Dai, Q., Bi, X., Song, W., Li, T., Liu, B., Ding, J., Xu, J., Song, C., Yang, N., Schulze, B. C., Zhang, Y., Feng, Y., and Hopke, P. K.: Residential coal combustion as a source of primary sulfate in Xi'an, China, *Atmospheric Environment*, 196, 66-76, 10.1016/j.atmosenv.2018.10.002, 2019.

778

Ding, J., Zhao, P., Su, J., Dong, Q., Du, X., and Zhang, Y.: Aerosol pH and its driving factors in Beijing,

779 Atmospheric Chemistry and Physics, 19, 7939-7954, 10.5194/acp-19-7939-2019, 2019.

780 Du, Q., Zhang, C., Mu, Y., Cheng, Y., Zhang, Y., Liu, C., Song, M., Tian, D., Liu, P., Liu, J., Xue, C., and

781 Ye, C.: An important missing source of atmospheric carbonyl sulfide: Domestic coal combustion,

782 Geophysical Research Letters, 43, 8720-8727, 10.1002/2016gl070075, 2016.

783 Fountoukis, C., and Nenes, A.: ISORROPIA II: a computationally efficient thermodynamic equilibrium

784 model for  $K^+$ - $Ca^{2+}$ - $Mg^{2+}$ - $NH_4^+$ - $Na^+$ - $SO_4^{2-}$ - $NO_3^-$ - $Cl^-$ - $H_2O$  aerosols, Atmospheric Chemistry and Physics,

785 7, 4639-4659, 2007.

786 Ge, X., He, Y., Sun, Y., Xu, J., Wang, J., Shen, Y., and Chen, M.: Characteristics and Formation

787 Mechanisms of Fine Particulate Nitrate in Typical Urban Areas in China, Atmosphere, 8, 62,

788 10.3390/atmos8030062, 2017.

789 Graedel, T. E., and Weschler, C. J.: Chemistry within aqueous atmospheric aerosols and raindrops,

790 Reviews of Geophysics, 19, 505-539, 10.1029/RG019i004p00505, 1981.

791 Guo, H., Xu, L., Bougiatioti, A., Cerully, K. M., Capps, S. L., Hite, J. R., Carlton, A. G., Lee, S. H.,

792 Bergin, M. H., Ng, N. L., Nenes, A., and Weber, R. J.: Fine-particle water and pH in the southeastern

793 United States, Atmospheric Chemistry and Physics, 15, 5211-5228, 10.5194/acp-15-5211-2015, 2015.

794 Guo, H., Weber, R. J., and Nenes, A.: High levels of ammonia do not raise fine particle pH sufficiently

795 to yield nitrogen oxide-dominated sulfate production, Scientific reports, 7, 12109, 10.1038/s41598-017-

796 11704-0, 2017.

797 Guo, S., Hu, M., Zamora, M. L., Peng, J., Shang, D., Zheng, J., Du, Z., Wu, Z., Shao, M., Zeng, L.,

798 Molina, M. J., and Zhang, R.: Elucidating severe urban haze formation in China, Proceedings of the

799 National Academy of Sciences of the United States of America, 111, 17373-17378,

800 10.1073/pnas.1419604111, 2014.

801 He, H., Wang, Y., Ma, Q., Ma, J., Chu, B., Ji, D., Tang, G., Liu, C., Zhang, H., and Hao, J.: Mineral dust

802 and  $NO_x$  promote the conversion of  $SO_2$  to sulfate in heavy pollution days, Scientific reports, 4, 1-5,

803 10.1038/srep04172, 2014.

804 He, P., Xie, Z., Chi, X., Yu, X., Fan, S., Kang, H., Liu, C., and Zhan, H.: Atmospheric  $\Delta 17O(NO_3^-)$

805 reveals nocturnal chemistry dominates nitrate production in Beijing haze, Atmospheric Chemistry and

806 Physics, 18, 14465-14476, 10.5194/acp-18-14465-2018, 2018.

807 Hennigan, C. J., Izumi, J., Sullivan, A. P., Weber, R. J., and Nenes, A.: A critical evaluation of proxy

808 methods used to estimate the acidity of atmospheric particles, Atmospheric Chemistry and Physics, 15,

809 2775-2790, 10.5194/acp-15-2775-2015, 2015.

810 Huang, R. J., Zhang, Y., Bozzetti, C., Ho, K. F., Cao, J. J., Han, Y., Daellenbach, K. R., Slowik, J. G.,

811 Platt, S. M., Canonaco, F., Zotter, P., Wolf, R., Pieber, S. M., Bruns, E. A., Crippa, M., Ciarelli, G.,

812 Piazzalunga, A., Schwikowski, M., Abbaszade, G., Schnelle-Kreis, J., Zimmermann, R., An, Z., Szidat,

813 S., Baltensperger, U., El Haddad, I., and Prevot, A. S.: High secondary aerosol contribution to particulate

814 pollution during haze events in China, Nature, 514, 218-222, 10.1038/nature13774, 2014.

815 Ibusuki, T., and Takeuchi, K.: Sulfur-dioxide oxidation by oxygen catalyzed by mixtures of manganese(II)

816 and iron(III) in aqueous-solutions at environmental reaction conditions, Atmospheric Environment, 21,

817 1555-1560, 10.1016/0004-6981(87)90317-9, 1987.

818 ~~Kuang, Y., Zhao, C. S., Ma, N., Liu, H. J., Bian, Y. X., Tao, J. C., and Hu, M.: Deliquescent phenomena~~

819 ~~of ambient aerosols on the North China Plain, Geophysical Research Letters, 43, 8744-8750,~~

820 ~~10.1002/2016gl070273, 2016.~~

821 Li, G., Bei, N., Cao, J., Huang, R., Wu, J., Feng, T., Wang, Y., Liu, S., Zhang, Q., Tie, X., and Molina, L.

822 T.: A possible pathway for rapid growth of sulfate during haze days in China, Atmospheric Chemistry

823 and Physics, 17, 3301-3316, 10.5194/acp-17-3301-2017, 2017.

824 Li, J., Liao, H., Hu, J., and Li, N.: Severe particulate pollution days in China during 2013-2018 and the  
825 associated typical weather patterns in Beijing-Tianjin-Hebei and the Yangtze River Delta regions,  
826 Environ Pollut, 248, 74-81, 10.1016/j.envpol.2019.01.124, 2019.

827 Li, L., Hoffmann, M. R., and Colussi, A. J.: Role of nitrogen dioxide in the production of sulfate during  
828 Chinese haze-aerosol episodes, Environ Sci Technol, 52, 2686-2693, 10.1021/acs.est.7b05222, 2018.

829 Li, Q., Li, X., Jiang, J., Duan, L., Ge, S., Zhang, Q., Deng, J., Wang, S., and Hao, J.: Semi-coke briquettes:  
830 towards reducing emissions of primary PM<sub>2.5</sub>, particulate carbon, and carbon monoxide from household  
831 coal combustion in China, Scientific reports, 6, 1-10, 10.1038/srep19306, 2016.

832 Liu, M., Song, Y., Zhou, T., Xu, Z., Yan, C., Zheng, M., Wu, Z., Hu, M., Wu, Y., and Zhu, T.: Fine particle  
833 pH during severe haze episodes in northern China, Geophysical Research Letters, 44, 1-9,  
834 10.1002/2017GL073210, 2017a.

835 Liu, P., Zhang, C., Mu, Y., Liu, C., Xue, C., Ye, C., Liu, J., Zhang, Y., and Zhang, H.: The possible  
836 contribution of the periodic emissions from farmers' activities in the North China Plain to atmospheric  
837 water-soluble ions in Beijing, Atmospheric Chemistry and Physics, 16, 10097-10109, 10.5194/acp-16-  
838 10097-2016, 2016a.

839 Liu, P., Zhang, C., Xue, C., Mu, Y., Liu, J., Zhang, Y., Tian, D., Ye, C., Zhang, H., and Guan, J.: The  
840 contribution of residential coal combustion to atmospheric PM<sub>2.5</sub> in northern China during winter,  
841 Atmospheric Chemistry and Physics, 17, 11503-11520, 10.5194/acp-17-11503-2017, 2017b.

842 ~~Liu, Q., Jing, B., Peng, C., Tong, S., Wang, W., and Ge, M.: Hygroscopicity of internally mixed multi-~~  
843 ~~component aerosol particles of atmospheric relevance, Atmospheric Environment, 125, 69-77,~~  
844 ~~10.1016/j.atmosenv.2015.11.003, 2016b.~~

845 Ma, Q., Wang, T., Liu, C., He, H., Wang, Z., Wang, W., and Liang, Y.: SO<sub>2</sub> Initiates the efficient  
846 conversion of NO<sub>2</sub> to HONO on MgO Surface, Environ Sci Technol, 51, 3767-3775,  
847 10.1021/acs.est.6b05724, 2017.

848 Meng, Z. Y., Lin, W. L., Jiang, X. M., Yan, P., Wang, Y., Zhang, Y. M., Jia, X. F., and Yu, X. L.:  
849 Characteristics of atmospheric ammonia over Beijing, China, Atmospheric Chemistry and Physics, 11,  
850 6139-6151, 10.5194/acp-11-6139-2011, 2011.

851 Murphy, J. G., Gregoire, P. K., Tevlin, A. G., Wentworth, G. R., Ellis, R. A., Markovic, M. Z., and  
852 VandenBoer, T. C.: Observational constraints on particle acidity using measurements and modelling of  
853 particles and gases, Faraday Discussions, 200, 379-395, 10.1039/c7fd00086c, 2017.

854 Nie, W., Ding, A., Wang, T., Kerminen, V. M., George, C., Xue, L., Wang, W., Zhang, Q., Petaja, T., Qi,  
855 X., Gao, X., Wang, X., Yang, X., Fu, C., and Kulmala, M.: Polluted dust promotes new particle formation  
856 and growth, Scientific reports, 4, 1-6, 10.1038/srep06634, 2014.

857 Pathak, R. K., Louie, P. K. K., and Chan, C. K.: Characteristics of aerosol acidity in Hong kong,  
858 Atmospheric Environment, 38, 2965-2974, 10.1016/j.atmosenv.2004.02.044, 2004.

859 ~~Ponczek, M., Hayeck, N., Emmelin, C., and George, C.: Heterogeneous photochemistry of dicarboxylic~~  
860 ~~acids on mineral dust, Atmospheric Environment, 212, 262-271, 10.1016/j.atmosenv.2019.05.032, 2019.~~

861 Quan, J., Tie, X., Zhang, Q., Liu, Q., Li, X., Gao, Y., and Zhao, D.: Characteristics of heavy aerosol  
862 pollution during the 2012-2013 winter in Beijing, China, Atmospheric Environment, 88, 83-89,  
863 10.1016/j.atmosenv.2014.01.058, 2014.

864 Ravishankara, A.: Heterogeneous and multiphase chemistry in the troposphere, Science, 276, 1058-1065,  
865 1997.

866 Seinfeld, J. H., and Pandis, S. N.: Atmospheric Chemistry and Physics, from Air Pollution to Climate

867 Change, Wiley, 429-443 pp., 2006.

868 Shao, J., Chen, Q., Wang, Y., Lu, X., He, P., Sun, Y., Shah, V., Martin, R. V., Philip, S., Song, S., Zhao,  
869 Y., Xie, Z., Zhang, L., and Alexander, B.: Heterogeneous sulfate aerosol formation mechanisms during  
870 wintertime Chinese haze events: air quality model assessment using observations of sulfate oxygen  
871 isotopes in Beijing, *Atmospheric Chemistry and Physics*, 19, 6107-6123, 10.5194/acp-19-6107-2019,  
872 2019.

873 Shi, G., Xu, J., Peng, X., Xiao, Z., Chen, K., Tian, Y., Guan, X., Feng, Y., Yu, H., Nenes, A., and Russell,  
874 A. G.: pH of aerosols in a polluted atmosphere: source contributions to highly acidic aerosol, *Environ*  
875 *Sci Technol*, 51, 4289-4296, 10.1021/acs.est.6b05736, 2017.

876 [Sun, Y., Wang, Z., Fu, P., Jiang, Q., Yang, T., Li, J., and Ge, X.: The impact of relative humidity on](#)  
877 [aerosol composition and evolution processes during wintertime in Beijing, China, \*Atmospheric\*](#)  
878 [Environment, 77, 927-934, 10.1016/j.atmosenv.2013.06.019, 2013.](#)

879 [Tang, M., Huang, X., Lu, K., Ge, M., Li, Y., Cheng, P., Zhu, T., Ding, A., Zhang, Y., Gligorovski, S.,](#)  
880 [Song, W., Ding, X., Bi, X., and Wang, X.: Heterogeneous reactions of mineral dust aerosol: implications](#)  
881 [for tropospheric oxidation capacity, \*Atmospheric Chemistry and Physics\*, 17, 11727-11777, 10.5194/acp-](#)  
882 [17-11727-2017, 2017.](#)

883 Tham, Y. J., Wang, Z., Li, Q., Wang, W., Wang, X., Lu, K., Ma, N., Yan, C., Kecorius, S., Wiedensohler,  
884 A., Zhang, Y., and Wang, T.: Heterogeneous N<sub>2</sub>O<sub>5</sub> uptake coefficient and production yield of ClNO<sub>2</sub> in  
885 polluted northern China: roles of aerosol water content and chemical composition, *Atmospheric*  
886 *Chemistry and Physics*, 18, 13155-13171, 10.5194/acp-18-13155-2018, 2018.

887 Tong, S. R., Hou, S. Q., Zhang, Y., Chu, B. W., Liu, Y. C., He, H., Zhao, P. S., and Ge, M. F.: Exploring  
888 the nitrous acid (HONO) formation mechanism in winter Beijing: direct emissions and heterogeneous  
889 production in urban and suburban areas, *Faraday Discussions*, 189, 213-230, 10.1039/c5fd00163c, 2016.

890 Wang, G., Zhang, R., Gomez, M. E., Yang, L., Levy Zamora, M., Hu, M., Lin, Y., Peng, J., Guo, S.,  
891 Meng, J., Li, J., Cheng, C., Hu, T., Ren, Y., Wang, Y., Gao, J., Cao, J., An, Z., Zhou, W., Li, G., Wang, J.,  
892 Tian, P., Marrero-Ortiz, W., Secret, J., Du, Z., Zheng, J., Shang, D., Zeng, L., Shao, M., Wang, W.,  
893 Huang, Y., Wang, Y., Zhu, Y., Li, Y., Hu, J., Pan, B., Cai, L., Cheng, Y., Ji, Y., Zhang, F., Rosenfeld, D.,  
894 Liss, P. S., Duce, R. A., Kolb, C. E., and Molina, M. J.: Persistent sulfate formation from London Fog to  
895 Chinese haze, *Proceedings of the National Academy of Sciences of the United States of America*, 113,  
896 13630-13635, 2016.

897 Wang, G., Zhang, F., Peng, J., Duan, L., Ji, Y., Marrero-Ortiz, W., Wang, J., Li, J., Wu, C., Cao, C., Wang,  
898 Y., Zheng, J., Secret, J., Li, Y., Wang, Y., Li, H., Li, N., and Zhang, R.: Particle acidity and sulfate  
899 production during severe haze events in China cannot be reliably inferred by assuming a mixture of  
900 inorganic salts, *Atmospheric Chemistry and Physics*, 18, 10123-10132, 10.5194/acp-18-10123-2018,  
901 2018a.

902 Wang, H., Lu, K., Chen, X., Zhu, Q., Wu, Z., Wu, Y., and Sun, K.: Fast particulate nitrate formation via  
903 N<sub>2</sub>O<sub>5</sub> uptake aloft in winter in Beijing, *Atmospheric Chemistry and Physics*, 18, 10483-10495,  
904 10.5194/acp-18-10483-2018, 2018b.

905 Wang, H., Lu, K., Guo, S., Wu, Z., Shang, D., Tan, Z., Wang, Y., Le Breton, M., Lou, S., Tang, M., Wu,  
906 Y., Zhu, W., Zheng, J., Zeng, L., Hallquist, M., Hu, M., and Zhang, Y.: Efficient N<sub>2</sub>O<sub>5</sub> uptake and NO<sub>3</sub>  
907 oxidation in the outflow of urban Beijing, *Atmospheric Chemistry and Physics*, 18, 9705-9721,  
908 10.5194/acp-18-9705-2018, 2018c.

909 Wang, J., Zhang, X., Guo, J., Wang, Z., and Zhang, M.: Observation of nitrous acid (HONO) in Beijing,  
910 China: Seasonal variation, nocturnal formation and daytime budget, *The Science of the total environment*,

911 587-588, 350-359, 10.1016/j.scitotenv.2017.02.159, 2017.

912 Wang, Y., Yao, L., Wang, L., Liu, Z., Ji, D., Tang, G., Zhang, J., Sun, Y., Hu, B., and Xin, J.: Mechanism  
913 for the formation of the January 2013 heavy haze pollution episode over central and eastern China,  
914 Science China Earth Sciences, 57, 14-25, 10.1007/s11430-013-4773-4, 2013.

915 Weber, R. J., Guo, H., Russell, A. G., and Nenes, A.: High aerosol acidity despite declining atmospheric  
916 sulfate concentrations over the past 15 years, Nature Geoscience, 9, 282-285, 10.1038/ngeo2665, 2016.

917 Wu, J., Bei, N., Hu, B., Liu, S., Zhou, M., Wang, Q., Li, X., Liu, L., Feng, T., Liu, Z., Wang, Y., Cao, J.,  
918 Tie, X., Wang, J., Molina, L. T., and Li, G.: Is water vapor a key player of the wintertime haze in North  
919 China Plain?, Atmospheric Chemistry and Physics, 19, 8721-8739, 10.5194/acp-19-8721-2019, 2019.

920 Xu, L., Duan, F., He, K., Ma, Y., Zhu, L., Zheng, Y., Huang, T., Kimoto, T., Ma, T., Li, H., Ye, S., Yang,  
921 S., Sun, Z., and Xu, B.: Characteristics of the secondary water-soluble ions in a typical autumn haze in  
922 Beijing, Environ Pollut, 227, 296-305, 10.1016/j.envpol.2017.04.076, 2017.

923 Xu, W. Y., Zhao, C. S., Ran, L., Deng, Z. Z., Liu, P. F., Ma, N., Lin, W. L., Xu, X. B., Yan, P., He, X., Yu,  
924 J., Liang, W. D., and Chen, L. L.: Characteristics of pollutants and their correlation to meteorological  
925 conditions at a suburban site in the North China Plain, Atmospheric Chemistry and Physics, 11, 4353-  
926 4369, 10.5194/acp-11-4353-2011, 2011.

927 Xue, C., Ye, C., Ma, Z., Liu, P., Zhang, Y., Zhang, C., Tang, K., Zhang, W., Zhao, X., Wang, Y., Song,  
928 M., Liu, J., Duan, J., Qin, M., Tong, S., Ge, M., and Mu, Y.: Development of stripping coil-ion  
929 chromatograph method and intercomparison with CEAS and LOPAP to measure atmospheric HONO,  
930 The Science of the total environment, 646, 187-195, 10.1016/j.scitotenv.2018.07.244, 2019a.

931 Xue, C., Ye, C., Zhang, Y., Ma, Z., Liu, P., Zhang, C., Zhao, X., Liu, J., and Mu, Y.: Development and  
932 application of a twin open-top chambers method to measure soil HONO emission in the North China  
933 Plain, Sci. Total Environ., 659, 621-631, 10.1016/j.scitotenv.2018.12.245, 2019b.

934 ~~Xue, J., Griffith, S. M., Yu, X., Lau, A. K. H., and Yu, J. Z.: Effect of nitrate and sulfate relative abundance  
935 in PM<sub>2.5</sub> on liquid water content explored through half hourly observations of inorganic soluble aerosols  
936 at a polluted receptor site, Atmospheric Environment, 99, 24-31, 10.1016/j.atmosenv.2014.09.049, 2014.~~

937 Xue, J., Yuan, Z., Griffith, S. M., Yu, X., Lau, A. K., and Yu, J. Z.: Sulfate Formation Enhanced by a  
938 Cocktail of High NO<sub>x</sub>, SO<sub>2</sub>, Particulate Matter, and Droplet pH during Haze-Fog Events in Megacities  
939 in China: An Observation-Based Modeling Investigation, Environ Sci Technol, 50, 7325-7334,  
940 10.1021/acs.est.6b00768, 2016.

941 Yang, T., Sun, Y., Zhang, W., Wang, Z., Liu, X., Fu, P., and Wang, X.: Evolutionary processes and sources  
942 of high-nitrate haze episodes over Beijing, Spring, J Environ Sci (China), 54, 142-151,  
943 10.1016/j.jes.2016.04.024, 2017.

944 Yang, Y. R., Liu, X. G., Qu, Y., An, J. L., Jiang, R., Zhang, Y. H., Sun, Y. L., Wu, Z. J., Zhang, F., Xu, W.  
945 Q., and Ma, Q. X.: Characteristics and formation mechanism of continuous hazes in China: a case study  
946 during the autumn of 2014 in the North China Plain, Atmospheric Chemistry and Physics, 15, 8165-8178,  
947 10.5194/acp-15-8165-2015, 2015.

948 Ye, C., Liu, P., Ma, Z., Xue, C., Zhang, C., Zhang, Y., Liu, J., Liu, C., Sun, X., and Mu, Y.: High H<sub>2</sub>O<sub>2</sub>  
949 Concentrations Observed during Haze Periods during the Winter in Beijing: Importance of H<sub>2</sub>O<sub>2</sub>  
950 Oxidation in Sulfate Formation, Environmental Science & Technology Letters, 5, 757-763,  
951 10.1021/acs.estlett.8b00579, 2018.

952 Zhang, H., Chen, S., Zhong, J., Zhang, S., Zhang, Y., Zhang, X., Li, Z., and Zeng, X. C.: Formation of  
953 aqueous-phase sulfate during the haze period in China: Kinetics and atmospheric implications,  
954 Atmospheric Environment, 177, 93-99, 10.1016/j.atmosenv.2018.01.017, 2018.

955 Zhang, Q., He, K. B., and Huo, H.: Cleaning China's air, *Nature*, 484, 161-162, 2012.

956 Zhang, R., Wang, G., Guo, S., Zamora, M. L., Ying, Q., Lin, Y., Wang, W., Hu, M., and Wang, Y.:  
957 Formation of urban fine particulate matter, *Chem Rev*, 115, 3803-3855, 10.1021/acs.chemrev.5b00067,  
958 2015.

959 Zhao, M., Wang, S., Tan, J., Hua, Y., Wu, D., and Hao, J.: Variation of Urban Atmospheric Ammonia  
960 Pollution and its Relation with PM<sub>2.5</sub> Chemical Property in Winter of Beijing, China, *Aerosol and Air*  
961 *Quality Research*, 16, 1390-1402, 10.4209/aaqr.2015.12.0699, 2016.

962 Zheng, B., Zhang, Q., Zhang, Y., He, K. B., Wang, K., Zheng, G. J., Duan, F. K., Ma, Y. L., and Kimoto,  
963 T.: Heterogeneous chemistry: a mechanism missing in current models to explain secondary inorganic  
964 aerosol formation during the January 2013 haze episode in North China, *Atmospheric Chemistry and*  
965 *Physics*, 15, 2031-2049, 10.5194/acp-15-2031-2015, 2015a.

966 Zheng, G. J., Duan, F. K., Su, H., Ma, Y. L., Cheng, Y., Zheng, B., Zhang, Q., Huang, T., Kimoto, T.,  
967 Chang, D., Pöschl, U., Cheng, Y. F., and He, K. B.: Exploring the severe winter haze in Beijing: the  
968 impact of synoptic weather, regional transport and heterogeneous reactions, *Atmospheric Chemistry and*  
969 *Physics*, 15, 2969-2983, 10.5194/acp-15-2969-2015, 2015b.

970 Zhong, J., Zhang, X., Wang, Y., Wang, J., Shen, X., Zhang, H., Wang, T., Xie, Z., Liu, C., Zhang, H.,  
971 Zhao, T., Sun, J., Fan, S., Gao, Z., Li, Y., and Wang, L.: The two-way feedback mechanism between  
972 unfavorable meteorological conditions and cumulative aerosol pollution in various haze regions of China,  
973 *Atmospheric Chemistry and Physics*, 19, 3287-3306, 10.5194/acp-19-3287-2019, 2019.

974

975